The *Sticta filix - Sticta lacera* conundrum (lichenized Ascomycota: Peltigeraceae subfamily Lobarioideae): unresolved lineage sorting or developmental switch?

ROBERT LÜCKING[1,3,*,⊠], BIBIANA MONCADA[1,2,3], TODD J. WIDHELM[3],
H. THORSTEN LUMBSCH[3], DAN J. BLANCHON[4] and PETER J. DE LANGE[4]

[1]*Botanischer Garten (Bo), Freie Universität Berlin, Berlin 14195, Germany*
[2]*Licenciatura en Biología, Universidad Distrital Francisco José de Caldas, Torre de Laboratorios, Herbario, Bogotá D.C., Colombia*
[3]*Science & Education, The Field Museum, 1400 South Lake Shore Drive, Chicago, IL 60605, USA*
[4]*Applied Molecular Solutions Research Centre, School of Environmental and Animal Sciences, Unitec Institute of Technology, Auckland 1025, New Zealand*

We assessed the status of two New Zealand endemic morphodemes in the genus *Sticta*, currently treated as two separate taxa, *Sticta filix* and *Sticta lacera*. Both are green-algal lichens with a distinct stipe that grow in forested habitats and are suitable indicators of the indigenous vegetation health in forest ecosystems in New Zealand. They exhibit different morphologies and substrate ecologies: *S. filix* forms rather robust thalli, often on exposed trunks of phorophytes, with erect stems distinctly emerging from the substrate, whereas *S. lacera* is a more delicate lichen growing near the base of trees, usually among bryophyte mats or sheltered in the exposed portions of the phorophyte root-plate, with a prostrate, branched, stolon-like stem barely emerging from the substrate. Throughout their range, both taxa grow sympatrically and often in close proximity (syntopically). Despite the differences, ITS barcoding does not support the two morphodemes as separate species. In this study we assessed two possible explanations: (1) *S. filix* and *S. lacera* are discrete phenotypes of a single species, caused by developmental switching triggered by a discrete environmental variable, the propagules developing either on bare substrate or between bryophytes; and (2) the two morphodemes represent separate lineages, but ITS does not provide sufficient resolution to reflect this. We performed a quantitative analysis of morphological and ecological parameters, based on vouchered herbarium collections and field observations on iNaturalist NZ (https://inaturalist.nz), to assess the level of discreteness of the growth forms and to test for a correlation with the presence of a bryophyte mat. We further took advantage of an existing molecular data set from a target capture approach, comprised of 205 protein markers. This data set was used to establish a framework of percentage identities between pairs of the same and of different species among lobarioid Peltigeraceae and then to test whether the *S. filix/lacera* pairing fell closer to a within-species or a between-species pairing. The morphometric analysis of herbarium material resolved *S. filix* and *S. lacera* as two discrete morphs with little overlap, supported by numerous observations on iNaturalist NZ. However, whereas herbarium material suggested a significant association of the *lacera* morph with bryophyte mats, no such pattern was evident from field images on iNaturalist NZ, in which both morphs frequently associated with bryophyte mats. This highlights the limitations of herbarium material to correctly assess substrate ecology, whereas iNaturalist NZ postings had issues with correct identifications, given that especially *S. lacera* is easily confused with *Pseudocyphellaria multifida*. Based on the target capture data, the percentage identity of the *S. filix/lacera* pairing (99.43%) was significantly higher than that of all 12 between-species pairings (93.20–98.01%); it was at the same time lower than that of all within-species pairings (99.63–99.99%) but significantly so only in comparison with five out of the eight within-species pairings. The target capture approach is thus inconclusive, but the combination of all data suggests that *S. filix* and *S. lacera* are not discrete morphodemes of a single species but represent two separate lineages which emerged recently and hence cannot be resolved using the ITS barcoding marker or even a deeper phylogenomic approach based on protein-coding markers. We propose transplantation experiments and the application of RADseq to further assess this situation.

*Corresponding author. E-mail: r.luecking@bgbm.org

INTRODUCTION

The former family Lobariaceae, now subsumed as subfamily Lobarioideae in Peltigeraceae (Kraichak *et al.*, 2018; Lücking, 2019; Lumbsch & Leavitt, 2019), include conspicuous macrolichens mostly found in wet forests and alpine habitats (Galloway, 2007; de Lange & Galloway, 2015; Devkota *et al.*, 2017). Among the 13 currently accepted genera (Lücking *et al.*, 2017a; Widhelm *et al.*, 2018, 2019; Simon *et al.*, 2020), *Sticta* (Schreb.) Ach. is the largest, with *c.* 200 accepted species and > 500 predicted species (Lücking *et al.*, 2017a; Simon *et al.*, 2018a, b). *Sticta* is also highly diverse in biological terms, including species with either green algal or cyanobacterial photobionts, or both, and with variable morphology and reproductive modes (Galloway, 2007; Makryi, 2008; Moncada *et al.*, 2014a, b; Widhelm *et al.*, 2018).

The *Sticta filix* (Sw.) Nyl. morphodeme includes species with green algae and a basal stipe or 'holdfast' (Galloway, 2007), although species with this morphology are not necessarily closely related. The *S. filix* morphodeme is a characteristic element of wet forests in the Southern Hemisphere (Galloway, 1985, 2007; Galloway *et al.*, 1995). In New Zealand, four taxa are distinguished, namely *S. filix*, *Sticta lacera* (Hook.f. & Taylor) Müll.Arg., *Sticta latifrons* A.Rich. and *Sticta menziesii* Hook.f. & Taylor (Galloway, 1985, 2007; Ranft *et al.*, 2018). *Sticta filix*, *S. latifrons* and *S. menziesii* form conspicuous lichens with large thalli, their main stems emerging from the substrate. *Sticta filix* differs from the other two species by its frequently branched, highly dissected lobes. All three species have dendriscocauloid cyanomorphs (Ranft *et al.*, 2018). *Sticta lacera* resembles *S. filix* in the highly dissected lobes, but it forms rather small lichens, with thalli barely larger than 2 cm; the stem is typically proliferating, similar to a stolon, and only the side branches emerge from the substrate. In addition, *S. lacera* has a glabrous underside, whereas *S. filix* is typically thinly tomentose (Galloway, 1985, 2007). All four taxa are promising monitors of environmental health in New Zealand forest ecosystems, but at different levels of sensitivity, and their accurate taxonomy is indispensable for this purpose (Ranft *et al.*, 2018; de Lange *et al.*, 2018).

As part of an ongoing integrative taxonomic study of New Zealand Lobarioideae (Ranft *et al.*, 2018), ITS barcoding of New Zealand representatives of the *S. filix* morphodeme showed that the broad concept of *S. latifrons* adopted by Galloway (1997, 2007) included another

species, *S. menziesii*, which has now been reinstated (Ranft *et al.*, 2018). The same study revealed a further, distinct species so far only known by its dendriscocauloid cyanomorph, *Sticta dendroides* (Nyl.) Moncada, Lücking & de Lange. On the other hand, three specimens representing *S. lacera*, including one identified by the late David Galloway (Thomas *et al.*, 2002), clustered within *S. filix*, raising the possibility that *S. lacera* may not be a separate taxon, but perhaps represents a dwarf form of *S. filix* (Ranft *et al.*, 2018). However, the ITS barcoding locus may not provide sufficient resolution to address species delimitation if lineages diverged recently (Leavitt *et al.*, 2016). A prominent example in *Sticta* are the two well-known, cosmopolitan taxa *Sticta fuliginosa* (Dicks.) Ach. and *Sticta limbata* (Sm.) Ach. They are not separable using ITS sequence data (Moncada *et al.*, 2014a; Magain & Sérusiaux, 2015; Widhelm *et al.*, 2018, 2019), but have clearly disparate morphologies, one producing laminal isidia and the other chiefly marginal soralia (Galloway, 2007; Ekman *et al.*, 2019).

Discrete variation, especially in sympatric taxa, is usually taken as an indication for the presence of distinct lineages, even if ITS may not provide sufficient resolution (Magain *et al.*, 2017). However, another explanation for discrete variation is developmental switching, in which environmental triggers determine whether individuals of the same population and genotype develop one discrete morph or another (Lively, 1986; Moran, 1992; Weigel & Nilsson, 1995; West-Eberhard, 2003; Chevin & Lande, 2013; Futuyma, 2015; Chevin & Hoffmann, 2017; Sieriebriennikov *et al.*, 2018). This phenomenon could explain mismatches between phenotype and lineage assignment in species complexes (Muggia *et al.*, 2008, 2014; Lumbsch & Leavitt, 2011; Leavitt *et al.*, 2011; Boluda *et al.*, 2019). An eye-catching example among lichen fungi are photomorphs in which the same fungus, even the same individual, develops highly disparate thallus morphologies in association with either green algae or cyanobacteria (Armaleo & Clerc, 1991; Laundon, 1995; Heiðmarsson *et al.*, 1997; Jørgensen, 1998; Purvis, 2000; Stenroos *et al.*, 2003; Takahashi *et al.*, 2006; Goward, 2009; Högnabba *et al.*, 2009). In this case, the photobiont provides the 'environmental' trigger. Photomorphs are common in *Sticta* and its relatives in Peltigeraceae, including in the group under study (Tønsberg & Holtan-Hartwig, 1983; Sanders, 2001; Tønsberg & Goward, 2001; Galloway, 2007; Magain *et al.*, 2012; Moncada *et al.*, 2013; Tønsberg *et al.*, 2016; Ranft *et al.*, 2018), and so the potential for discrete variation has been demonstrated at least in *S. filix*.

To assess whether the *S. filix* and *S. lacera* morphs represent separate lineages or a potential case of developmental switching, we first increased sampling of the *S. lacera* morphodeme and assembled an emended phylogenetic tree based on the ITS barcoding locus, to see whether the previously found pattern is consistent. We further used a phylogenomic target capture approach (Coissac *et al.*, 2016; Greshake *et al.*, 2016; Pizarro *et al.*, 2018), taking advantage of a larger data set generated for another study (Widhelm *et al.*, 2019) that included the two target taxa. Here, we reanalysed these data to test a new approach of a pairwise percentage identity framework to decide whether two samples represent the same or two different species. Finally, we analysed the morphology and substrate ecology of vouchered herbarium specimens to quantitatively assess the level of discrete variation and its potential correlation with microenvironmental parameters, particularly substrate. This approach was complemented by an evaluation of field observations of the two taxa available on iNaturalist NZ (https://inaturalist.nz).

MATERIAL AND METHODS

ITS BARCODING AND HAPLOTYPE NETWORK

We obtained fresh material of two additional specimens of the *S. lacera* morphodeme, for a total of 12 specimens corresponding to *S. filix*, five to *S. lacera* and one to a dendriscocauloid cyanomorph, including 16 previously sequenced specimens. Using the methodology described in Ranft *et al.* (2018), we generated ITS barcoding sequences for the additional specimens for a total of 18 ingroup ITS accessions and performed maximum likelihood tree search using the universal GTR+Gamma model in RAxML 8.2 (Stamatakis, 2015). Following Ranft *et al.* (2018), *S. latifrons* was used as an outgroup (Table 1). To visualize multidimensional variation in the ITS, we computed a TCS haplotype network using PopART 1.7 (Clement *et al.*, 2002; Leigh & Bryant, 2015).

QUANTITATIVE MORPHOMETRY

This approach was applied to both the sequenced material and to herbarium specimens that were unfortunately too old to generate sequence data. For the sequenced specimens we assessed four characters considered diagnostic for *S. lacera* vs. *S. filix* (Galloway, 1985, 2007): thallus size (distance from base to tip of longest branch in cm), underside tomentum development (absent, present except lobe tips, fully present), stipe length (in cm) and proliferation of the main stem (absent, present; Supporting Information, Table S1). The matrix was analysed by means of

Table 1. Voucher specimens used in the ITS barcoding approach. Newly generated sequences are indicated in boldface. For voucher information on previously published sequences, see Thomas *et al.* (2002) and Ranft *et al.* (2018). Voucher material of the specimens collected on the North Island (Ranft *et al.*, 2018; this paper) is deposited in the herbaria AK (Auckland), B (Berlin), F (Chicago) and/or UNITEC (Auckland).

Taxon	Voucher	ITS accession
Dendriscocauloid cyanomorph	South Island	AF350303
Sticta filix	South Island	AF350304
Sticta filix	North Island	MF373759
Sticta filix	North Island	MF373769
Sticta filix	North Island	MF373770
Sticta filix	North Island	MF373771
Sticta filix	North Island	MF373772
Sticta filix	North Island	MF373773
Sticta filix	North Island	MF373774
Sticta filix	North Island	MF373775
Sticta filix	North Island	MF373776
Sticta filix	North Island	MF373777
Sticta filix	North Island	MF373779
Sticta lacera	South Island	AF350305
Sticta lacera	North Island	MF373766
Sticta lacera	North Island	MF373780
Sticta lacera	North Island, *de Lange 13439* (MON-5716)	**OL873582**
Sticta lacera	North Island, *de Lange 13690* (MON-5718)	**OL873583**
Sticta latifrons	South Island	AF350307
Sticta latifrons	North Island	MF373763
Sticta latifrons	North Island	MF373764
Sticta latifrons	North Island	MF373765
Sticta latifrons	North Island	MF373781
Sticta latifrons	North Island	MF373782
Sticta latifrons	North Island	MF373783
Sticta latifrons	North Island	MF373784
Sticta latifrons	North Island	MF373785
Sticta latifrons	North Island	MF373786

non-metric multidimensional scaling (NMDS) and cluster analysis, using the Euclidean distance and Ward's clustering method in PC-ORD 6.0 (McCune & Mefford, 2006). The sequenced dendriscocauloid cyanomorph was excluded from this analysis, as were two previously sequenced specimens of *S. filix* and *S. lacera* from the South Island (Thomas *et al.*, 2002), as we were unable to locate the underlying voucher material at the OTA herbarium (Otago) to assess their phenotypes. The same analysis was subsequently

performed on an additional 94 non-sequenced herbarium specimens from both the North Island and the South Island (Supporting Information, Table S1). For the NMDS ordination, we computed the axis correlation in the ordination diagram of the presence of a bryophyte mat as assessed in the dried collections.

FIELD OBSERVATIONS

Whereas direct field observations were available for the sequenced material, the ecological context, in particular association with bryophyte mats, of herbarium specimens could only be indirectly assessed, with the possibility of type II errors (false negative) in the case of *S. filix* since the latter is easily collected without associated bryophytes even if emerging from a bryophyte mat. We therefore complemented this approach with an assessment of field images provided by iNaturalist IZ (Mugford *et al.*, 2021) for *S. filix* (https://inaturalist.nz/observations?taxon_id=197044) and *S. lacera* https://inaturalist.nz/observations?taxon_id=408333). The limitations of this approach largely lie in the reliability of image-based identifications (Mugford *et al.*, 2021), which in the case of *S. filix* and *S. lacera* are complicated by superficially highly similar species in the related genus *Pseudocyphellaria* Vain., particularly *Pseudocyphellaria multifida* (Laurer) D.J.Galloway & P.James. Each of the entries was therefore first assessed for correct identification and subsequently the presence of a bryophyte mat over the substrate was recorded where possible given the angle of the field image. We also assessed whether the thallus consisted of few, large, emerging stems or numerous small branches close to the substrate, suggesting a proliferating main stem (see images linked in Supporting Information, Table S2).

TARGET CAPTURE APPROACH

The data for the target capture approach were taken from Widhelm *et al.* (2019), selecting *S. filix* and *S. lacera* and two samples each of six other Lobarioideae [*Pseudocyphellaria corbettii* D.J.Galloway, *Pseudocyphellaria dissimilis* (Nyl.) D.J.Galloway & P.James, *Pseudocyphellaria haywardiorum* D.J.Galloway, *Sticta fuliginosa*, *S. latifrons*, *Yoshimuriella peltigera* (Delise) Moncada & Lücking] plus one of *Yarrumia coronata* (Müll.Arg.) D.J.Galloway and three of *Yarrumia colensoi* (C.Bab.) D.J.Galloway (Table 2). This selection represented species for which either two separate samples or samples of two related species (assessed from published taxonomies and ITS data) were available. In contrast to Widhelm *et al.* (2019), who focused on a phylogenomic approach to resolve the backbone of lobarioid Peltigeraceae, here we used a subset of the data to examine percentage identity between selected samples, to test whether a framework of between- and within-species thresholds can be established that would help to assess the situation in *S. filix* vs. *S. lacera*. The methodological details to obtain the capture data are fully outlined in Widhelm *et al.* (2019) and are here only briefly summarized as follows. Baits for target capture were designed using MarkerMiner 1.0 (Chamala *et al.*, 2015). We used the *Lobaria pulmonaria* (L.) Hoffm. genome to develop a custom database and Trinity (Grabherr *et al.*, 2011) to assemble transcriptome data from *Evernia prunastri* (L.) Ach., *Pseudevernia furfuracea* (L.) Zopf and *Lasallia pustulata* (L.) Mérat, to identify clusters of single-copy gene transcripts in the transcriptome assemblies. Using MarkerMiner, 1714 single-copy genes were identified and aligned to the hard-masked *L. pulmonaria* reference genome, from which loci were selected that had at least one exon of at least 500 bp and clear intron-exon boundaries on the hard-masked alignment. Baits were designed for using 400 separate Fasta DNA sequence files each from the *L. pulmonaria* and the *E. prunastri* genome. The sequences were submitted to MYcroarray (Arbor Biosciences, Ann Arbor, MI, USA) for MYbaits bait design, with 100-nucleotide-long baits with two times tiling density, resulting in 17 941 baits.

Library preparations were prepared from DNA isolated with the ZR Fungal/Bacterial DNA MiniPrep (Zymo Research, Irvine, CA, USA). DNA concentration was quantified with a Qubit 4 fluorometer (Thermo Fisher Scientific, Waltham, MA, USA). DNA fragments *c.* 500 bp were generated with a M220 Focused-Ultrasonicator (Woburn, MA, USA), cleaning the product with SeraPure beads (Glenn *et al.*, 2019). Samples were tagged using an Adapterama dual-indexing system (Glenn *et al.*, 2019) with a KAPA Hyper Prep Kit (KAPABiosystems, Wilmington, MA, USA). Ligation products were subjected to bead-based size selection with SeraPure beads to enrich for fragments of *c.* 550 bp, subsequently eluted in resuspension buffer (RSB) and used in a limited-cycle PCR to attach the tagged iTru5 and iTru7 Adapterama primers. PCR products were cleaned with 1× SeraPure beads and eluted in nuclease-free, PCR-grade water.

Samples were pooled by phylogenetic relatedness, corresponding to major clades in a previously published, three-locus phylogenetic tree for Lobarioideae (Moncada *et al.*, 2013), for hybridization with RNA baits. For each sample, DNA was mixed with all samples of each of the five pools and concentrated in a heated vacuum centrifuge. Pools were hybridized with reagents provided with the baits from MYcroarray. After incubation, the baits were attached to streptavidin beads and washed according to the MYcroarray protocol, followed by a post-wash enrichment PCR cycle with KAPA Hifi Hotstart ReadyMix. The products

Table 2. Voucher specimens used in the target capture approach, representing a subset of the sampling analysed by Widhelm *et al.* (2019). Voucher specimens are deposited in the herbaria AK, B, F, and/or UNITEC (for acronyms, see Table 1). SRA = Sequence Read Archive

Taxon	Number	SRA accession	Region	Locality	Voucher
Pseudocyphellaria corbettii	15893	SAMN10603063	New Zealand, North Island	Manawatu-Wanganui, Tongariro National Park	*Grewe & Wildhelm 3109*
Pseudocyphellaria corbettii	15903	SAMN10603073	New Zealand, North Island	Bay of Plenty, Kaimai Mamaku Forest Park	*Grewe et al. 3105*
Pseudocyphellaria dissimilis	14829	SAMN10602990	Australia	Tasmania, Mt. Field National Park	*Lumbsch et al. 2173*
Pseudocyphellaria dissimilis	15896	SAMN10603066	New Zealand, North Island	Auckland, Auckland City, Northshore, Birkdale, Eskdale Bush Preserve	*Grewe & Wildhelm 3019*
Pseudocyphellaria haywardiorum	15874	SAMN10603045	New Zealand, North Island	Central Volcanic Plateau, Tongariro National Park	*de Lange 12586 (AK 3575377)*
Pseudocyphellaria haywardiorum	15875	SAMN10603046	New Zealand, North Island	Central Volcanic Plateau, Tongariro National Park	*de Lange 12587 (AK 3575378)*
Sticta filix	15900	SAMN10603070	New Zealand, North Island	Kaimai, Bay of Plenty, Mamaku Forest Park	*Grewe et al. 3074*
Sticta fuliginosa	15880	SAMN10603051	New Zealand, Chatham Islands	Rekohu, Southern Tablelands, Alfred Preece's Land	*de Lange CH-2542 (UNITEC 7725)*
Sticta fuliginosa	15881	SAMN10603052	New Zealand, North Island	Eastern Wairarapa, Castlepoint Road	*de Lange 13163*
Sticta lacera	15902	SAMN10603072	New Zealand, North Island	Waikato, Kaimanawa Forest Park	*Grewe & Wildhelm 3255*
Sticta latifrons	15879	SAMN10603050	New Zealand, Chatham Islands	Rekohu, Hokorereoro/ Rangatira/ South East Island	*de Lange CH-2534 (UNITEC 7446)*
Sticta latifrons	15901	SAMN10603071	New Zealand, North Island	Wellington, Tararua Forest Park	*Grewe & Wildhelm 3274*
Yarrumia colensoi	15316	SAMN10603016	New Zealand, North Island	Hawke's Bay, Mahia Peninsula Scenic Reserve	*Lücking et al. 38741*
Yarrumia colensoi	15851	SAMN10603038	New Zealand, North Island	Waikato, Tongariro National Park	*Lücking et al. 38836*
Yarrumia colensoi	15317	SAMN10603017	New Zealand, North Island	Waikato, Western Bay Road, Great Lake Trail Waihaha Link	*Lücking et al. 38974*
Yarrumia coronata	15850	SAMN10603037	New Zealand, North Island	Hawke's Bay, Mahia Peninsula Scenic Reserve	*Lücking et al. 38675*
Yoshimuriella peltigera	15279	SAMN10603013	Colombia, Cundinamarca	Subachoque, El Tablazo	*Rivera 60*
Yoshimuriella peltigera	15280	SAMN10603014	Colombia, Cundinamarca	Subachoque, El Tablazo	*Rivera & Salinas 127*

Abbreviation: SRA, Sequence Read Archive.

were cleaned with 1× SeraPure beads and the DNA concentration was quantified with a Qubit fluorometer and size of distribution of the DNA fragments in the pools was observed on an Agilent 2001 Bioanalyzer (Santa Clara, CA, USA). The pools were mixed in a final 96-sample pool, for sequencing on the Field Museum's Pritzker Laboratory's Illumina MiSeq, with a single 300-cycle v.2 MiSeq reagent kit (Illumina, San Diego, CA, USA). Data processing was performed as described in detail in Widhelm *et al.* (2019).

Hybpiper (Johnson *et al.*, 2016) was used to generate coding sequences from raw sequencing reads (see Widhelm *et al.*, 2019). The BLASTX option was used to map sequencing reads with an amino acid sequence target file that was generated from the *Lobaria pulmonaria* transcriptome on the JGI Genome Portal (https://genome.jgi.doe.gov/portal). Sequences from the 18 specimens were recovered for 224 loci producing 224 unaligned multi-FASTA files. Each of the 224 data sets was aligned using the auto option in MAFFT 7 (Katoh & Standley, 2013). Each alignment was subsequently manually inspected and problematic sequence data were classified into: (1) low quality, (2) potential chimeras, (3) with terminal gaps, (4) with indels and (5) missing for a particular sample. Low quality sequences and potential chimeras were removed. Four of the 224 alignments required manual adjustments. After checking, we retained 205 marker alignments that were complete for the target specimens (Supporting Information, File S3).

Pairings of samples corresponding to the target taxa were extracted from the full alignments using SAMtools 1.12 (Li *et al.*, 2009), resulting in 4305 alignments with two samples each (21 pairings of 205 loci each). Samples were paired as follows to obtain reference comparisons for within-species and between-species pairings:

- Within species (eight pairings): *Pseudocyphellaria corbettii*, *P. dissimilis*, *P. haywardiorum*, *Sticta fuliginosa*, *S. latifrons*, *Yarrumia colensoi* (two combinations out of three specimens), *Yoshimuriella peltigera*.
- Among species (closely related based on ITS; five pairs with two pairings each): *Pseudocyphellaria corbettii* vs. *P. dissimilis*, *P. corbettii* vs. *P. haywardiorum*, *Sticta latifrons* vs. *S. lacera*, *S. latifrons* vs. *S. filix*, *Yarrumia colensoi* vs. *Y. coronata*.
- Between species (distantly related based on ITS; one pair with two pairings): *Sticta latifrons* vs. *S. fuliginosa*.

The two-sequence alignments were imported into Geneious 10 (Kearse *et al.*, 2012) and the percent identity for each of the alignments was extracted into a csv file consisting of gene name, sample pairing and percent pairwise identity of the two sequences in each of the 4305 alignments. The resulting data file was used to produce density ridge plots in R using the packages *ggplot2* (Wickham, 2016), *ggridges* (Wilke, 2017) and *viridis* (Garnier, 2016). One-way analysis of variance (ANOVA) was used to compare the mean percent identities of 205 gene alignments for each infraspecific and intraspecific species pair. The R package *dplyr* (Wickham *et al.*, 2015) was used

to conduct the ANOVA. The null hypothesis assumed that *S. lacera*/*S. filix* represent a single species, with the mean percent sequence identity not differing significantly from other within-species pairings but significantly from between-species pairings.

RESULTS

ITS BARCODING

The ITS barcoding locus (alignment length: 540 bases) revealed mostly identical sequences for both morphs, with few, mostly autapomorphic variations in two sequences of *S. filix* from the North Island (Ranft *et al.*, 2018: MF373771, MF373771: one position or 0.2%), one sequence of *S. filix* and *S. lacera* each from the South Island (Thomas *et al.*, 2002: AF350304, AF350305: three positions each or 0.6%) and one sequence corresponding to a dendriscocauloid cyanomorph from the South Island (Thomas *et al.*, 2002: AF350303: one position or 0.2%). All other sequences, including four of *S. lacera* and nine of *S. filix* from the North Island, were identical (Fig. 1). Three out of four unique haplotypes, including the two most distinctive haplotypes, came from the South Island, including both morphodemes and the dendriscocauloid cyanomorph, indicating that the variation in ITS is correlated with geography rather than phenotype. Consequently, the best-scoring maximum likelihood tree did not resolve the two morphodemes as separate lineages (Fig. 2).

QUANTITATIVE MORPHOMETRY

Morphometric analysis of the sequenced specimens resulted in a clear separation of the two morphs (Fig.
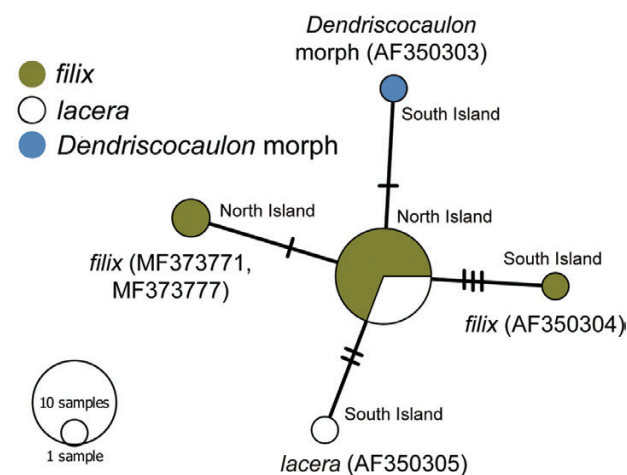

Figure 1. ITS haplotype network of the *Sticta filix-lacera* complex in New Zealand. Tick lines indicate number of base call differences between haplotypes.
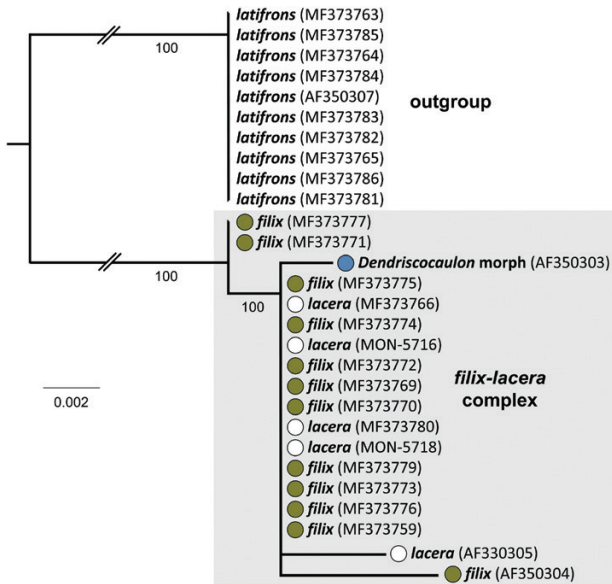
Figure 2. Best-scoring maximum likelihood tree for the ITS barcoding marker of the *Sticta filix-lacera* complex in New Zealand. Bootstrap support values are indicated below the branches.

3A, B), corresponding to the concept of *S. filix* (11 specimens) and *S. lacera* (four specimens). Among these sequenced specimens, the *S. filix* morph had thalli 50–80 mm long (mean 67 ± 9 mm), with the lobe underside thinly tomentose except for the lobe margins or glabrous except for the central stem, and a stipe 10–20 mm long (mean 13 ± 5 mm), without proliferations (Fig. 4). In contrast, the *S. lacera* morph had thalli (i.e. emerging branches) 20–30 mm long (mean 26 ± 5 mm), with the lobe underside glabrous and a stipe 5–10 mm long (mean 6 ± 3 mm), consistently proliferating (Fig. 5). There were no intermediate specimens.

Morphometric analysis including additional herbarium specimens revealed a more complex picture (Figs 6, 7). In the NMDS ordination, the two morphs were dispersed along a gradient, slightly overlapping in the first plane (axis 1 vs. 2; Fig. 6, insert) but more distinctly separated in the second plane (axis 1 vs. 3; Fig. 6). The *S. filix* morph exhibited a higher degree of variation than the *S. lacera* morph. Among these specimens, the *S. filix* morph had thalli 40–125 mm large (mean 72 ± 21 mm) and a stipe 3–30 mm long (mean 11 ± 6 mm). The *S. lacera* morph had thalli (i.e. emerging branches) 6–32 mm large (mean 19 ± 7 mm) and a stipe 0–6 mm long (mean 1 ± 1 mm). In the cluster analysis (Fig. 7), the *S. lacera* morph formed two groups, one containing most specimens (group A) and a small one comprised of four specimens (group B). Both groups were nested in a more heterogeneous cluster of specimens corresponding to

the *S. filix* morph, forming three larger groups and two singletons. Notably, in that larger analysis, the previously separated sequenced specimens (Fig. 3A, B) formed two tight clusters, well separated from each other (Fig. 7), demonstrating that the morphological analysis based on the sequenced specimens alone was misleading. In particular, the sequenced specimens of the *S. filix* morphodeme were characterized by rather short stems and stipes compared to the non-sequenced material (Supporting Information, Table S1).

The NMDS ordination revealed a significant correlation of specimens arranged by morphological characters with the presence/absence of a bryophyte mat, the group of specimens corresponding to the *S. lacera* morph showing an association with the presence of such mats (Fig. 6). Indeed, only 29% of the *filix* specimens had associated bryophytes, compared to 97% of the *lacera* specimens (Supporting Information, Table S1), a highly significant difference (Chi-square test; $\chi^2 = 16.9016$, $P = 0.0000$). Three of the four morphological characters (thallus size, lower side tomentum, stipe size) showed some level of variation, including slight overlap between the morphodeme groups separated by the cluster analysis, whereas the fourth character (stem proliferation) was an almost perfect indicator of both the larger clusters and the two morphodemes (Fig. 7).

Analysis of the two morphometric characters, stem length and stipe length, showed that the variation in the two morphodemes is not actually continuous. Stem length exhibited a rather clear bimodal distribution, whereas stipe length was multimodal, with a broader, somewhat discontinuous variation found in specimens corresponding to the *S. filix* morphodeme (Fig. 8).

FIELD OBSERVATIONS

We assessed a total of 114 postings of either *S. filix* (92) or *S. lacera* (22) on iNaturalist NZ, including two where both morphs were present. Critical evaluation confirmed the identifications for 65 postings of *S. filix* and 13 postings of *S. lacera*, one each including both species, for 66 and 14 records, respectively. Identification accuracy thus amounted to 71% for *S. filix* and 59% for *S. lacera*. The remaining records represented in part *Pseudocyphellaria* spp., particularly *P. multifida*, lichens not identifiable to species or genus level due to lack of critical diagnostic information (e.g. the underside) and, in a few cases, potentially undescribed, additional species in the *S. filix* group (Supporting Information, Table S2). Among the verified identifications, the *S. filix* and *S. lacera* morphodemes were clearly separated, with no intermediate forms; in two cases (https://inaturalist.nz/observations/982725; https://inaturalist.nz/observations/19226970), both forms grew side by side
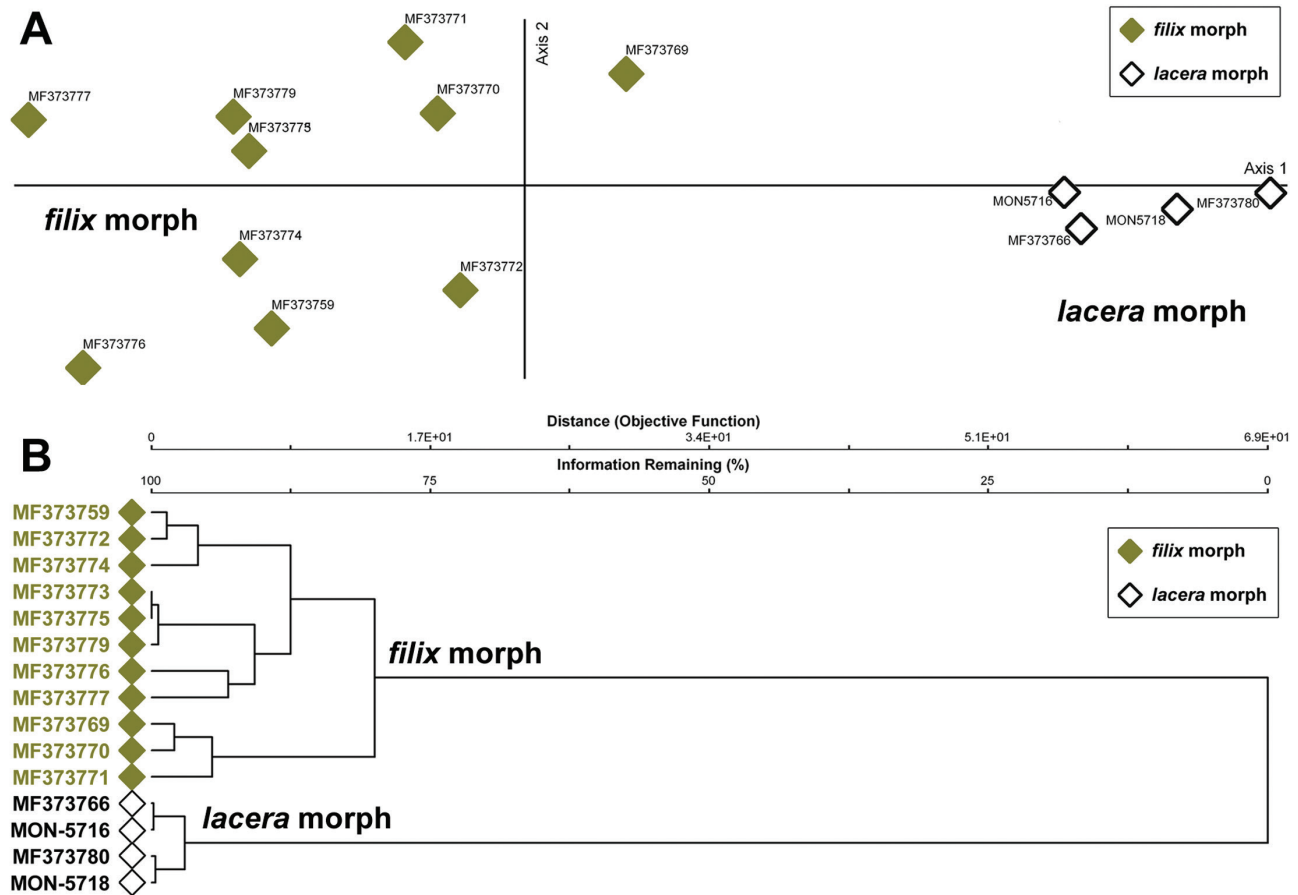
Figure 3. PCA ordination (A) and cluster analysis (B) of sequenced specimens corresponding to the *S. filix* and *S. lacera* morphs.

(syntopically) on the same substrate, a phenomenon also observed in other cases ([Fig. 9](#)). The presence or absence of a bryophyte mat could be assessed for 56 postings of *S. filix* and 13 of *S. lacera*. In contrast to the findings from the herbarium material, among the field observations *S. filix* was more frequently association with a bryophyte mat (68% of all records) than *S. lacera* (54%; [Fig. 10](#)). This difference was, however, not significant (Chi-square test; $\chi^2 = 0.913$, $P = 0.3393$).

TARGET CAPTURE APPROACH

For the eight pairings in which the paired samples represented a single species, mean genetic identity varied between 99.99% (*Yoshimuriella peltigera*) and 99.63–99.67% (*Pseudocyphellaria dissimilis*, *Sticta latifrons*, *Yarrumia colensoi p.p.*), with 99.82% or higher for the remaining three pairings ([Fig. 11](#); [Table 3](#)). For the five pairings representing different but closely related species, mean genetic identity ranged between 98.00–98.01% (*P. corbettii* vs. *P. dissimilis*) and

96.90–96.95% (*P. corbettii* vs. *P. haywardiorum*), whereas for the pairing representing two more distantly related species (*S. fuliginosa* vs. *S. latifrons*), mean genetic identity was 93.10–93.20% ([Fig. 11](#); [Table 3](#)). There was a slight effect of geographical distance: the five within-species pairings with the highest percentage similarity included two instances of pairings from the same locality, two from different localities on the same island and only one from two distant regions (*S. fuliginosa* from the North Island and from the Chatham Islands); in contrast, the three pairings with lower percentage similarity included one instance from two distant regions (*P. dissimilis* from Australia and New Zealand) and two from different localities on the same island (*S. latifrons*, *Yarrumia colensoi*; [Fig. 11](#)). For the pairing *S. filix* vs. *S. lacera*, mean genetic identity was 99.43%, lower than any within-species but higher than any between-species pairing ([Fig. 11](#); [Table 3](#)). For between-species pairings of the same taxa but different specimens, mean genetic identity varied little, between 0.01% in *P. corbettii* vs. *P. dissimilis* and 0.10% in *S. latifrons* vs. *S. fuliginosa* and *Yarrumia coronata* vs. *Yarrumia colensoi* ([Table 3](#)).
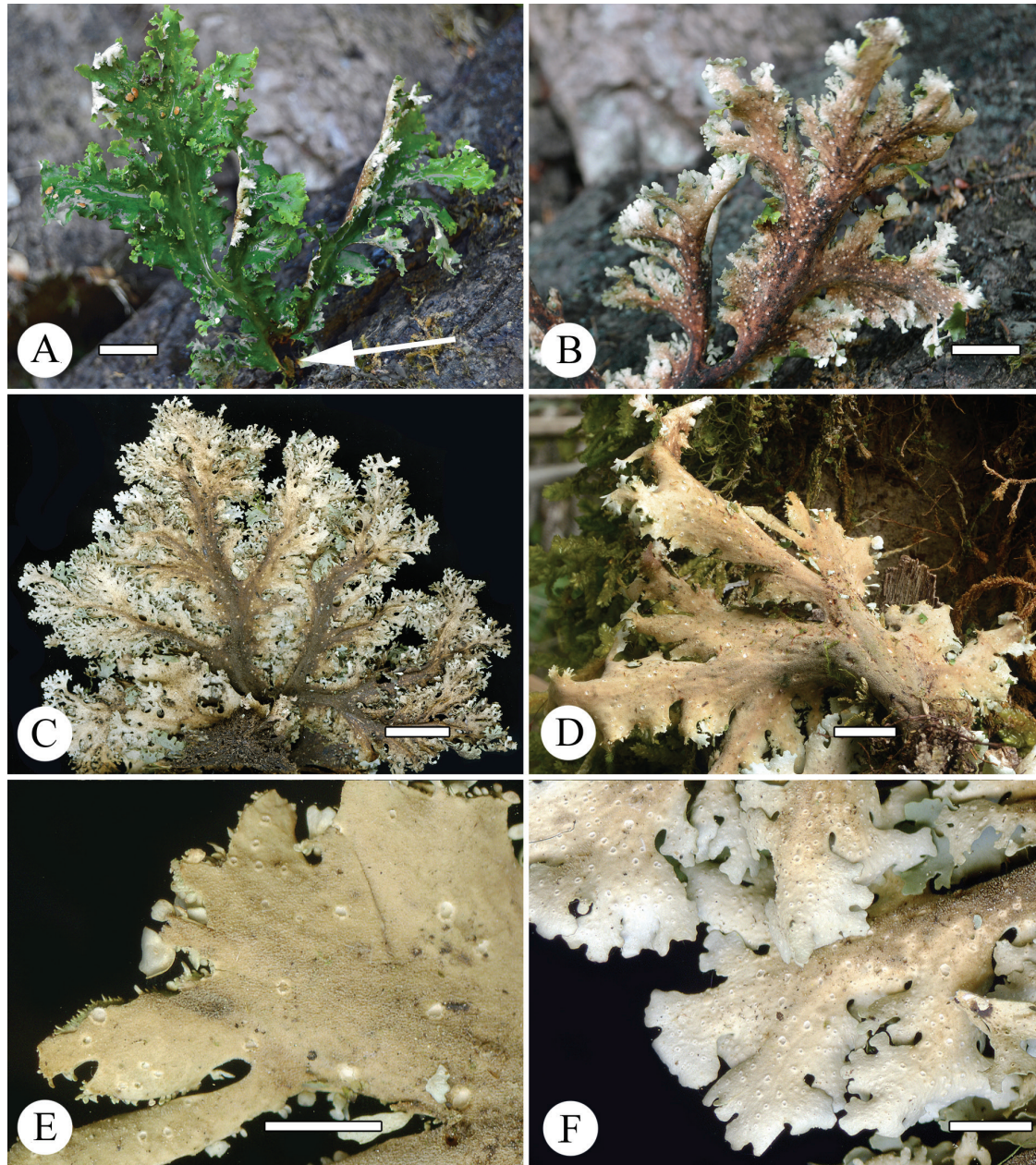
Figure 4. Morphology of sequenced specimens corresponding to the *S. filix* morph. A, B, thallus upper and lower side of ITS accession MF373770; the arrow in A indicates the basal stipe, i.e. the distance from the substrate to the first branch. C, thallus lower side of ITS accession MF373776; in both cases showing dendroid morph with distinct central stem and terminal lobules with glabrous underside. D, E, thallus lower side of ITS accession MF373773; dendroid morph lacking distinct central stem, with the lobe underside thinly tomentose throughout. F, thallus lower side of ITS accession MF373777; specimen showing nearly glabrous lobe underside, with tomentum only developed towards the central stem. Scale bar = 10 mm (A-D), = 5 mm (E, F).

Tukey post hoc comparison revealed highly significant differences in the pairwise genetic identity between the two samples representing the *S. filix* vs. *S. lacera* morphodeme and all between-species pairings (Table 3). Five of the eight within-species pairs also had mean pairwise identities significantly different from those of

S. filix vs. *S. lacera*, whereas the remaining three did not differ significantly (Table 3). The *S. filix* vs. *S. lacera* pairing was thus closer to a within-species than to a between-species identity pattern. However, even though the two samples originated from different localities of the same island (North Island), the percentage identity
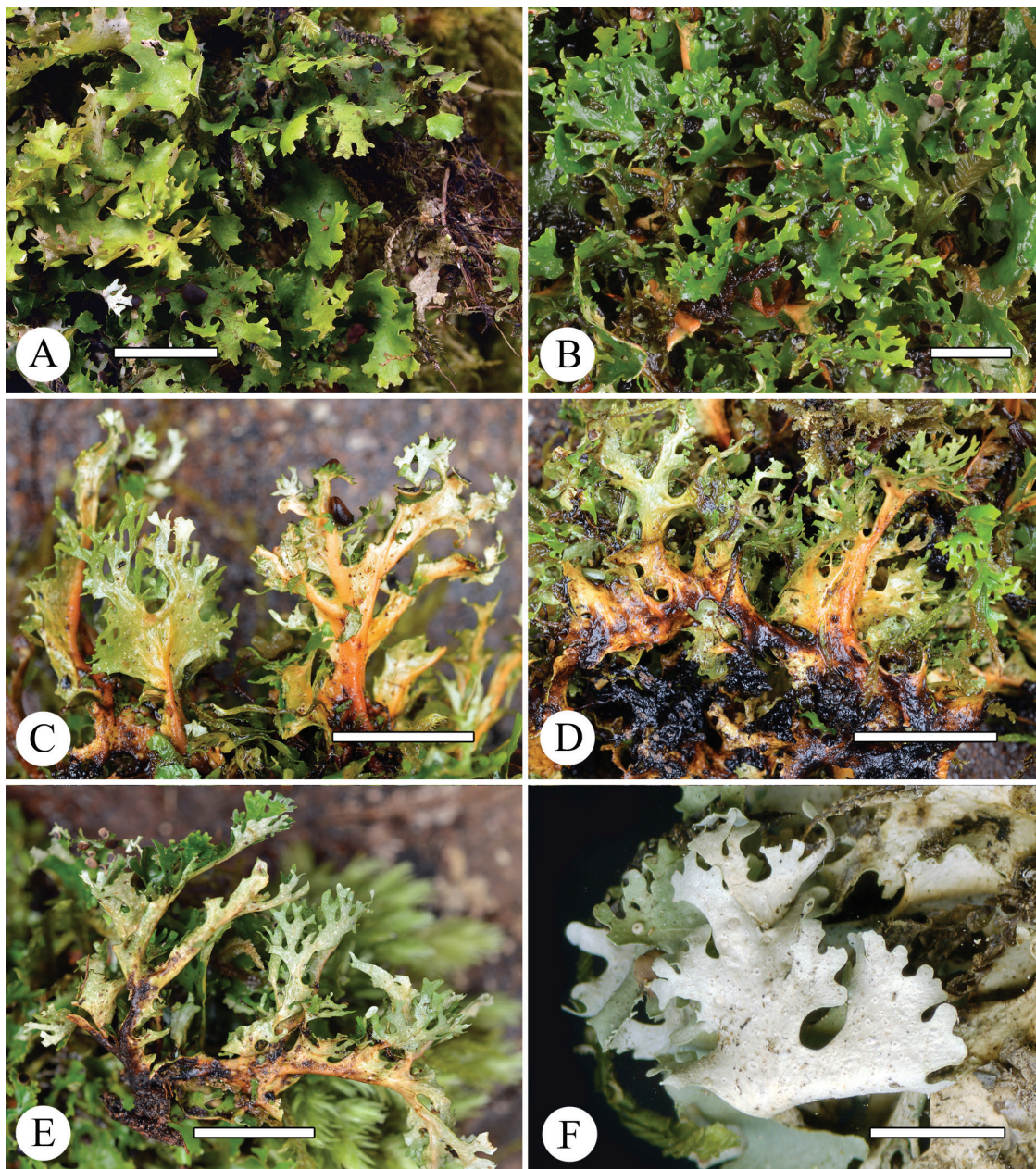
Figure 5. Morphology of sequenced specimens corresponding to the *S. lacera* morph. A, thallus upper side of ITS accession MF373780. B, thallus upper side of *Lücking 38158*; in both cases mats of small stems growing between bryophytes (mosses). C, D, individual branches of proliferating stem removed from bryophyte mat of *Lücking 38158*. E, individual branches of proliferating stem removed from bryophyte mat of ITS accession MON-5716; in both cases stems removed showing basal connection to a procumbent, proliferating portion of the stem (stipe) that subsequently often disintegrates. F, thallus lower side of ITS accession MF373780; glabrous lobe underside closely resembling that of lobe tips of the *S. filix* morph (compare Fig. 4F). Scale bar = 10 mm (A-E), = 5 mm (F).

was lower than the two most similar within-species pairings (*P. dissimilis*, *S. latifrons*), both originating from distant regions (Fig. 11), which implies that the percentage identity in the *S. filix*/*S. lacera* pairing is lower than expected given their geographical distance, if both represented the same species.

DISCUSSION

Given the absence of resolution in the ITS barcoding marker, the discrete morphodemes corresponding to *S. filix* and *S. lacera* allow for two possible explanations. A frequently employed scenario would
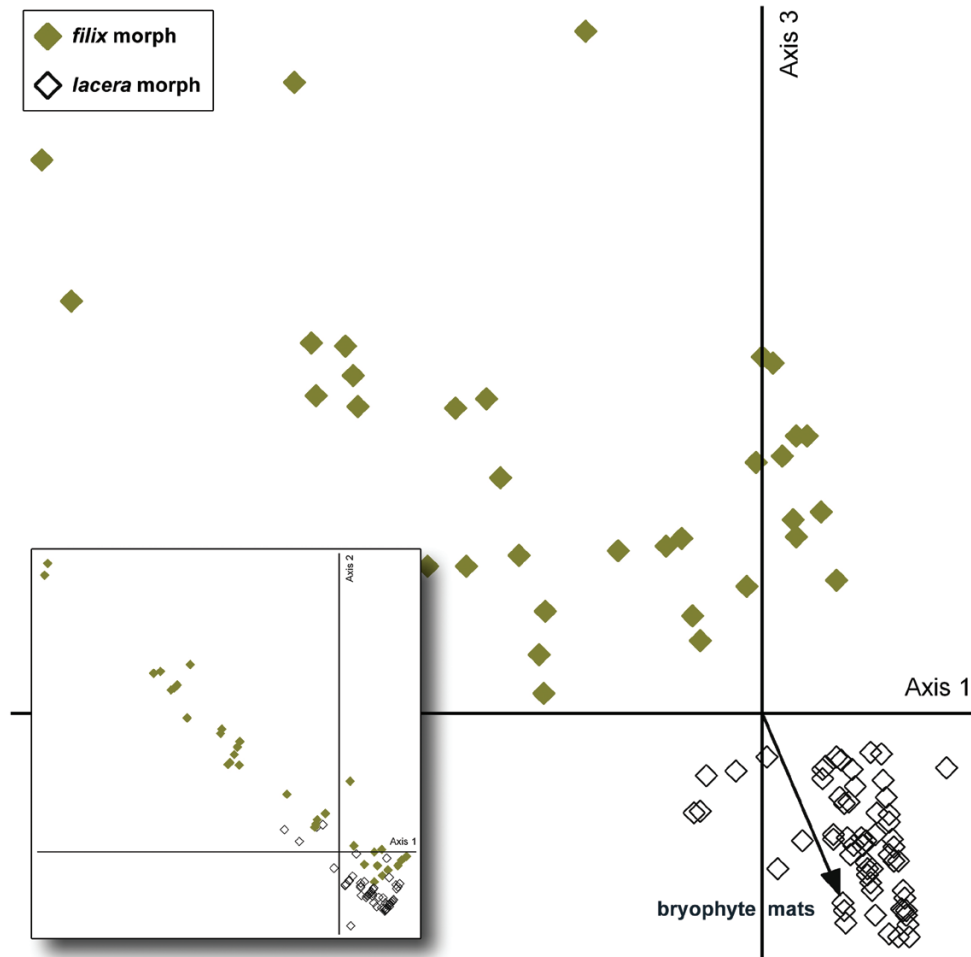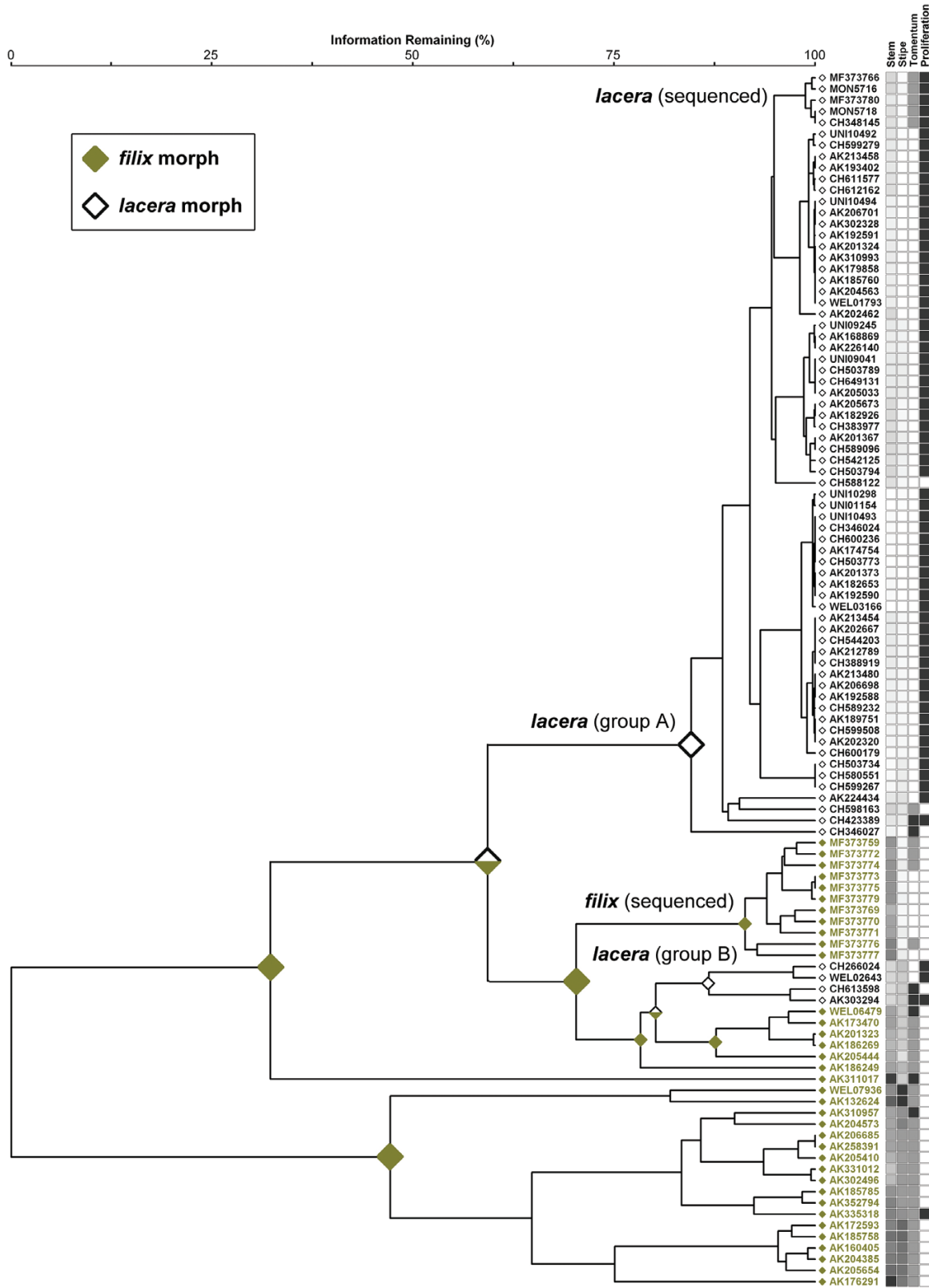
Figure 6. NMDS ordination of 109 specimens corresponding to the *S. filix* and *S. lacera* morphs, based on four morphological characters. Specimens were assigned to morphs based on the key provided by Galloway (2007). The larger graph shows the second plane (axis 1 vs. 3) and the smaller inset shows the first plane (axis 1 vs. 2). The arrow indicates a significant correlation of the second plane axes with the presence/absence of bryophyte mats.

be the assumption that *S. filix* and *S. lacera* are two separate species, but with the ITS barcoding locus insufficient to resolve this relationship, because the species have evolved recently from a common ancestor (Magain *et al.*, 2017; Ranft *et al.*, 2018). ITS has indeed been shown to be rather conserved in certain lineages of fungi, such as *Aspergillus* Micheli, *Fusarium* Link, *Pseudocercospora* (Lév.) Speg. or *Schizophyllum* Fr., with other markers better resolving species-level lineages (James *et al.*, 2001; Eberhardt, 2010; Crous *et al.*, 2013; Samson *et al.*, 2014; O'Donnell *et al.*, 2015). In Lobarioideae, ITS generally works well in delimiting species, with both single marker and multilocus approaches (Moncada *et al.*, 2013, 2014a, b; Cornejo & Scheidegger 2015; Lücking *et al.*, 2017b; Ranft *et al.*, 2018; Simon *et al.*, 2018a). However, a notable exception is the clade including the two cosmopolitan species, *S. fuliginosa*

and *S. limbata*, which are clearly distinguishable morphologically, including differential vegetative reproductive strategies (isidia vs. soredia), but cannot be resolved using ITS (Moncada *et al.*, 2014a; Magain & Sérusiaux, 2015; Widhelm *et al.*, 2018).

One would expect a phylogenomic approach to be able to resolve closely related species-level lineages if the ITS barcoding marker lacks such resolving power. However, even the target capture approach, based on 205 different markers, was not conclusive in this case. Although the genetic identity of the *S. filix*/*S. lacera* pairing was lower than those of all eight within-species pairings, representing four genera of Lobarioideae (*Pseudocyphellaria*, *Sticta*, *Yarrumia*, *Yoshimuriella*), the observed differences were only significant for five of these pairings. On the other hand, genetic identity of the *S. filix*/*S. lacera* pairing was distinctly higher than for all between-species pairings, in all cases

Figure 7. Cluster analysis of a large number of specimens corresponding to the *S. filix* and *S. lacera* morphs, based on four morphological characters. Specimens were assigned to morphs based on the key provided by Galloway (2007).
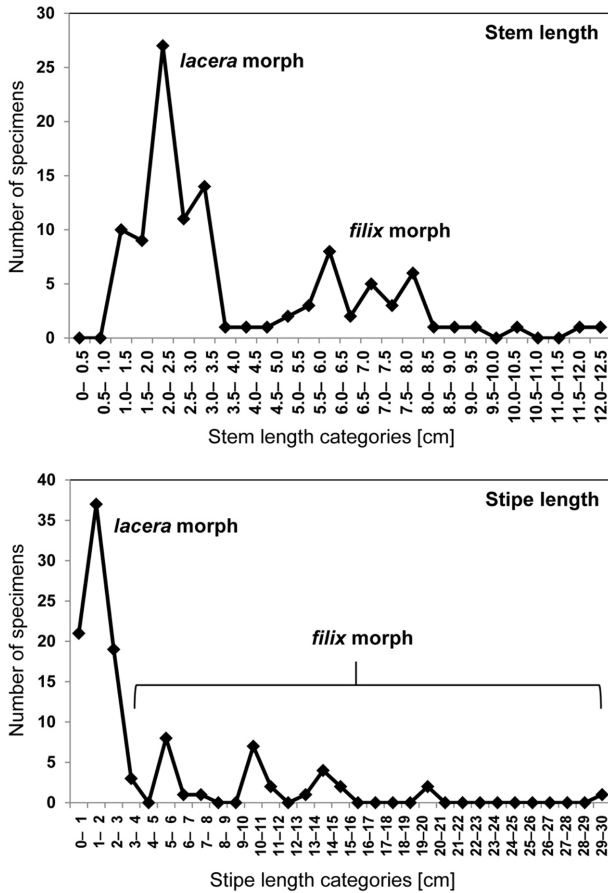
Figure 8. Variation of stem length and stipe length in the *S. filix* and *S. lacera* morphodemes.

significantly so. Statistically, it is therefore more likely that the *S. filix/S. lacera* pairing represents a single species. However, its placement at the lowermost level of the within-species gradient, and the fact that its percentage identity was lower than expected based on the geographical distance of the underlying samples compared to similar cases, indicate that this pairing may represent a recently emerged divergence, not readily reflected even in the target capture approach. More sensitive methods such as RADseq or microsatellite markers (Grewe *et al.*, 2018; Lagostina *et al.*, 2018; Widhelm *et al.*, 2021) are needed to further resolve this issue.

If the two morphs do not represent distinct taxa, the alternative scenario would postulate that material identified with either name represent discrete morphs of a single species, unrelated to genotype but triggered by environmental factors. Thus, *S. lacera* could be considered a form of *S. filix* in which the basal portion of the stem is procumbent and proliferates horizontally, supported by the substrate and hence remaining delicate and inconspicuous. In contrast, typical *S. filix*

Figure 9. Examples of *S. filix* and *S. lacera* growing syntopically. A, North Island, Hunua Range, Rata Track (https://inaturalist.nz/observations/19226970)] (photograph: P. de Lange). B, North Island, Ruahine Range (photograph provided by Allison Knight, reproduced with permission).

would develop the stipe and stem ascending from the substrate, with overarching branches. The notion that *S. filix* and *S. lacera* may represent a single taxon was supported by our finding that the perception
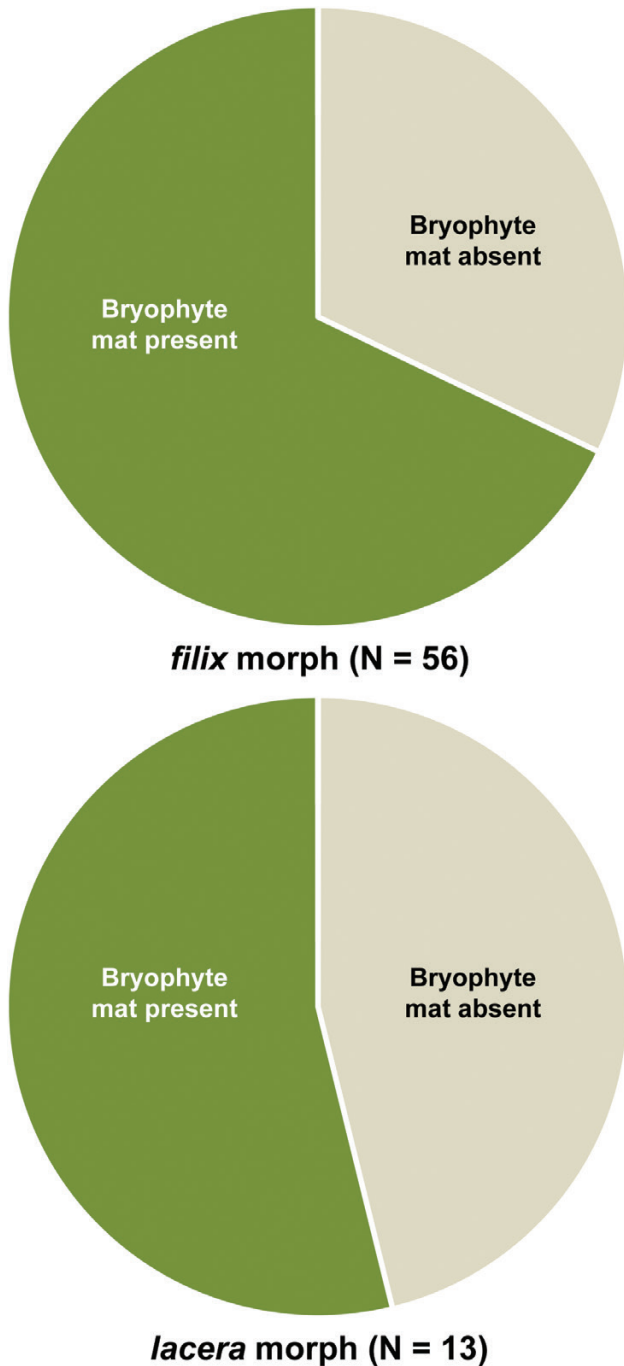
Figure 10. Proportion of specimens associated with basal bryophyte mats in *S. filix* and *S. lacera*, based on field observations posted on iNaturalist NZ (see Supporting Information, Table S2).

of *S. lacera* as a more delicate lichen is misguided: careful separation of the material from intermingled bryophytes revealed that the individuals are much larger than perceived by considering the separate, ascending stems only, the latter being attached to a

proliferating, procumbent part that would be analogous to the branched, erect stem of typical *S. filix*. The lobes and lobules were found to be identical in terms of their variation in both morphs, and the fact that in typical *S. filix* the lower tomentum was usually restricted to the stem and adjacent areas may explain why the underside in the *S. lacera* morph is entirely glabrous, as the 'stem' remains horizontal and hidden between bryophyte mats.

Morphological analysis of only the sequenced specimens of the *S. filix*/*S. lacera* complex supported the notion that the two morphodemes are strongly discrete. However, inclusion of a much larger number of non-sequenced herbarium collections rendered this pattern more complex, the presumably diagnostic characters exhibiting some level of overlap, particularly the development of the lower side tomentum, but also stipe and stem length. Still, the observed variation was not that of a morphologically continuous population, and multivariate analysis resolved discrete entities. This was also supported by the field observations posted on iNaturalist NZ, which allowed to readily assign all verified records to either morphodeme. Multivariate and comparative statistical analysis is often applied to support species-level delimitations in the absence of molecular data (Lutzoni, 1994; Tretiach & Hafellner, 1998; Llop & Gómez-Bolea, 1999; Doré *et al.*, 2006), and it plays a central role in numerical taxonomy (Sneath & Sokal, 1973; Frisvad, 1992; Sieber *et al.*, 1998). However, discrete entities detected with such an approach are not necessarily proof of the existence of separate lineages.

Discordance between phenotype and molecularly defined lineages is not rare in lichen-forming fungi and has also been reported for other members of Peltigeraceae (Magain *et al.*, 2017, 2018). However, in cases where discrete morphodemes are not resolved molecularly, there is usually an explanation, such as a different reproductive mode, a different photobiont or a clear environmental trigger. Alternatively, especially in island biota, morphological differentiation may be more pronounced than genetic differentiation, with radiations classified into numerous species and even genera often showing genetic variation corresponding to populations in mainland taxa (Baldwin *et al.*, 1991; Baldwin & Sanderson, 1998; Carlquist *et al.*, 2003). In the New Zealand vascular flora, this has been found in species-rich or morphologically variable genera, e.g. *Alseuosmia* A.Cunn., *Epilobium* L., *Myosotis* L. and *Kunzea* Rchb. (Lorimer, 2007; Meudt *et al.*, 2014; de Lange, 2014; Shepherd *et al.*, 2019; L.D. Shepherd, pers. comm.), species of which exhibit morphological disparity and are widely sympatric or even syntopic, often forming hybrid swarms in sites of prolonged human disturbance, but which maintain their distinctiveness in natural systems where they
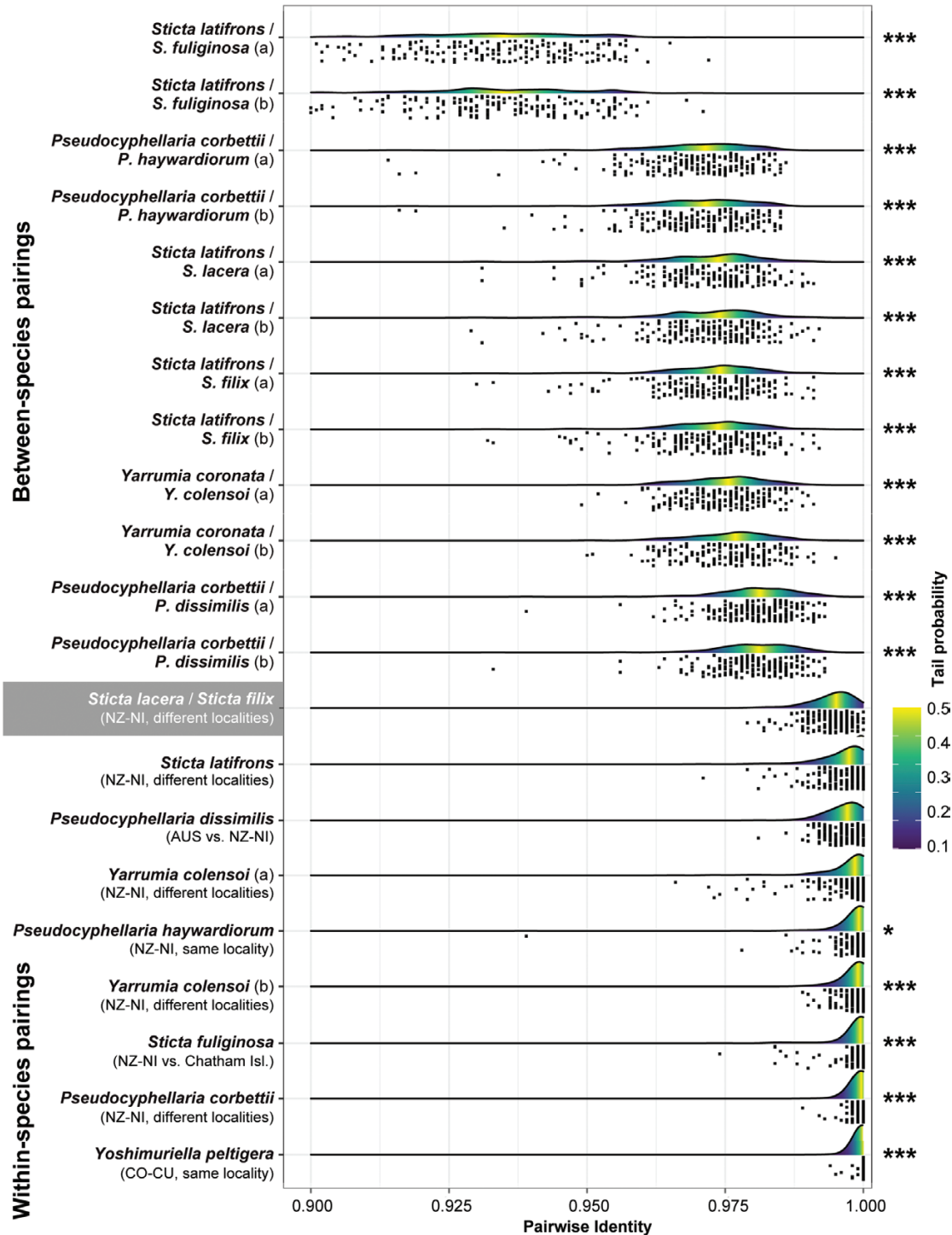
Figure 11. Distribution of genetic similarities of 205 markers in within- and between-species comparisons of selected species of Lobarioideae, including the *S. filix* vs. *S. lacera* morphodeme, based on a target capture approach. For exact percentage identity values see Table 3. Asterisks indicate whether a given pairing differed significantly from the *S. filix/S. lacera* pairing (* = significant at $P < 0.05$, *** = significant at $P < 0.001$). For within-species pairings, the geographic origin of the two samples is indicated, whether from the same locality, different localities on the same island, or remote localities on different islands or countries. Abbreviations: AUS, Australia; CO-CU, Colombia (Cundinamarca); NI, North Island; NZ, New Zealand.

Table 3. Tukey post hoc comparison of mean genetic distances of 205 markers between specimens of the *S. filix* vs. *S. lacera* morphodeme (99.43%) with mean genetic distances of selected other Lobarioideae pairings, including within- and between-species comparisons. Significant (*) and highly significant (***) differences between *S. filix*/ *S. lacera* and all other pairings are highlighted

Comparison	Species/pair compared to	Similarity (%)	Difference	Lower	Upper	*P*-value
Within-species	*Pseudocyphellaria corbettii*	99.93	−0.0050	−0.0083	−0.0017	**0.0000******
Within-species	*Pseudocyphellaria dissimilis*	99.65	−0.0023	−0.0055	0.0010	0.6497
Within-species	*Pseudocyphellaria haywardiorum*	99.82	−0.0039	−0.0072	−0.0006	**0.0037****
Within-species	*Sticta fuliginosa*	99.86	−0.0044	−0.0077	−0.0011	**0.0004******
Within-species	*Sticta latifrons*	99.63	0.0020	−0.0013	0.0053	0.8217
Within-species	*Yarrumia colensoi* (a)	99.67	0.0025	−0.0008	0.0058	0.4580
Within-species	*Yarrumia colensoi* (b)	99.85	0.0042	0.0010	0.0075	**0.0008******
Within-species	*Yoshimuriella peltigera*	99.99	0.0056	0.0023	0.0089	**0.0000******
Between-species	*P. corbettii* vs. *P. dissimilis* (a)	98.01	0.0142	0.0109	0.0175	**0.0000******
Between-species	*P. corbettii* vs. *P. dissimilis* (b)	98.00	0.0143	0.0110	0.0176	**0.0000******
Between-species	*P. corbettii* vs. *P. haywardiorum* (a)	96.90	0.0252	0.0220	0.0285	**0.0000******
Between-species	*P. corbettii* vs. *P. haywardiorum* (b)	96.95	0.0247	0.0214	0.0280	**0.0000******
Between-species	*S. latifrons* vs. *S. filix* (a)	97.25	−0.0076	−0.0109	−0.0043	**0.0000******
Between-species	*S. latifrons* vs. *S. filix* (b)	97.23	−0.0220	−0.0253	−0.0187	**0.0000******
Between-species	*S. latifrons* vs. *S. fuliginosa* (a)	93.20	−0.0633	−0.0666	−0.0620	**0.0000******
Between-species	*S. latifrons* vs. *S. fuliginosa* (b)	93.10	−0.0622	−0.0655	−0.0589	**0.0000******
Between-species	*S. latifrons* vs. *S. lacera* (a)	97.20	−0.0223	−0.0256	−0.0190	**0.0000******
Between-species	*S. latifrons* vs. *S. lacera* (b)	97.21	−0.0221	−0.0254	−0.0189	**0.0000******
Between-species	*Yarrumia coronata* vs. *Yarrumia colensoi* (a)	97.48	−0.0184	−0.0217	−0.0151	**0.0000******
Between-species	*Yarrumia coronata* vs. *Yarrumia colensoi* (b)	97.58	−0.0195	−0.0228	−0.0162	**0.0000******

behave as stable, 'functional' species. For such cases, until fully understood, sensible taxonomic resolution should remain morphology based. In Hawaii, this phenomenon has been documented for lichen formers in the lobarioid Peltigeraceae, in particular the genera *Lobariella* Yoshim. and *Pseudocyphellaria* (Moncada *et al.*, 2014b; Lücking *et al.*, 2017c).

Discrete phenotypic variation or polymorphism unrelated to genotype is assumed to be caused by developmental switches, in which environmental triggers early in the ontogeny determine whether an individual develops one form or the other. This phenomenon has been extensively investigated in animals, which are characterized by a closed body plan (Lively, 1986; Moran, 1992; Chevin & Lande, 2013; Futuyma, 2015; Chevin & Hoffmann, 2017; Sieriebriennikov *et al.*, 2018). In plants and fungi including lichens, which have an open body plan, discrete polymorphism is less well studied (Weigel & Nilsson, 1995), also because it often cannot be readily quantified. In lichens, the 'environmental trigger' may be the type of photobiont, e.g. whether a green alga or a cyanobacterium (Tønsberg & Holtan-Hartwig, 1983; Armaleo & Clerc, 1991; Laundon, 1995; Heiðmarsson *et al.*, 1997; Jørgensen, 1998; Purvis, 2000; Sanders, 2001; Tønsberg & Goward, 2001; Stenroos *et al.*, 2003; Takahashi *et al.*, 2006; Galloway, 2007; Goward, 2009; Högnabba *et al.*, 2009; Magain *et al.*, 2012; Moncada

et al., 2013; Tønsberg *et al.*, 2016; Ranft *et al.*, 2018). Even examples of disparate morphology in association with different green algae are known (Ertz *et al.*, 2018). These cases demonstrate that genetically identical lichen fungi can develop highly disparate thallus morphologies. Other examples of discrete phenotypical variation, including growth form and secondary chemistry, have been demonstrated in various groups of lichens (Muggia *et al.*, 2008, 2014; Lumbsch & Leavitt, 2011; Leavitt *et al.*, 2011, 2013; Fryday *et al.*, 2017; Boluda *et al.*, 2019). Also notable are so-called 'species pairs', morphologically identical forms that differ in their reproductive mode (Tehler, 1982; Mattsson & Lumbsch, 1989; Lohtander *et al.*, 1998; Myllys *et al.*, 2001; Articus *et al.*, 2002; Buschbom & Mueller, 2006; Crespo & Pérez-Ortega, 2009; Ludwig, 2011; Messuti *et al.*, 2016). Species pairs may represent the result of developmental switches early in the ontogeny that determine whether a particular individual produces ascomata or propagates vegetatively (Tehler, 1982; Ludwig, 2011).

Both *S. filix* and *S. lacera* propagate vegetatively with phyllidia, although apothecia producing ascospores are also common, especially in the former (Galloway, 2007). Both associate with green algae, but molecular data are thus far only available for *S. filix*, identifying the photobiont as *Elliptochloris* Tscherm.-Woess (Lindgren *et al.*, 2020). The other

two species in this group associate with *Elliptochloris* (*S. menziesii*) or *Heveochlorella* and *Chloridium* Link (*S. latifrons*), thus demonstrating differentiation in terms of photobiont associations among green algae between closely related mycobionts. In a more distantly related species, *S. subcaperata* (Nyl.) Nyl., the same mycobiont may associate with different photobionts, viz. *Elliptochloris*, *Heveochlorella* Zhang, Huss, Sun, Chang & Pang or *Chloridium* (Lindgren *et al.*, 2020), but the different photobionts do not trigger different thallus morphologies in that case, suggesting that differential green algal associations are not responsible for the morphological differences between the *S. filix* and *S. lacera* morphodeme. Given that among the three species of the *S. filix* group for which the photobiont is known, *S. latifrons* (with *Heveochlorella* or *Chloridium*) is more tolerant of disturbances (Ranft *et al.*, 2018), whereas species associated with *Elliptochloris* (*S. filix*, *S. menziesii*) are more confined to protected habitats, it is anyway likely that *S. lacera* has the same photobiont as *S. filix* (*Elliptochloris*).

The theoretical model underlying discrete, environmentally triggered variation or polymorphism assumes that the triggering variable is itself discrete. Leaving aside the photobiont, this would postulate discrete ecological differentiation. Both forms are ecologically partitioned: the *S. lacera* morphodeme typically prefers moist microhabitats, growing on logs, root bases and buttresses, sometimes even clay, usually amongst bryophytes. It is never found on exposed roots or higher up on trunks, a growth pattern more frequently seen in the *S. filix* morphodeme. However, this differentiation is far from discrete, as the two morphs often occur sympatrically and sometimes syntopically, leading back to our hypothesis that the presence of a bryophyte mat over the substrate may trigger the formation of the *S. lacera* morph during early thallus development. Our morpho-ecological analysis of numerous herbarium specimens would support this hypothesis, but no such correlation was found in the field observations assessed on iNaturalist NZ, thus contradicting the results based on the herbarium material and underlining the limitations of the latter when it comes to evaluations of ecological parameters. Although *S. filix* often emerges from basal bryophyte mats, it can be easily collected 'clean', and hence such an association would not be visible in herbarium samples. Another issue is that lichens grow more slowly than bryophytes, as their mycobiont biomass is non-photosynthetic, and so it is conceivable that bryophytes associated with mature thalli may not actually have been present when the lichen thallus became established. A further challenge to the explanation of a 'bryophyte trigger' is whether such a developmental switch would manifest itself differently

in sexual (ascospores) vs. vegetative (phyllidia) propagules, especially given that apothecia are more frequent in *S. filix* (Galloway, 2007). A conclusive test would be an approach through growth experiments with propagules of both forms using different substrate types.

Although developmental switches are theoretically uncorrelated with genotype and manifested in the phenotype through gene regulation (Sieriebriennikov *et al.*, 2018; Oettler *et al.*, 2019), they might provide a model of discrete polymorphism in ancestral populations that eventually may lead to sympatric speciation. The discrete morphodemes corresponding to *S. filix* and *S. lacera* correlate with ecological preferences that may cause reproductive isolation between the morphodemes, which in turn could lead to reproductive barriers at the genetic level if persisting long enough through time. Such isolation could lead to 'fixation' of certain morphodemes in descendant lineages. For instances, in *Sticta*, cyanobacterial photomorphs are the only known photomorphs in many lineages, apparently having lost the capability of producing a corresponding chloromorph (Lindgren *et al.*, 2020). Thus, the two alternative hypotheses, namely *S. filix* vs. *S. lacera* representing either a discrete dimorphism caused by a developmental switch or a recent lineage divergence not yet resolved, are not mutually exclusive but represent components of an evolutive scenario that would explain phenotypic and ecological divergence based on ancestral phenotypic polymorphism. Based on our findings, we therefore conclude that *S. filix* and *S. lacera* should be maintained as separate taxa, likely representing a case of active speciation that could serve as a model to investigate phenotypical and ecological differentiation in recently diverging lineages.

The mean genetic identities resulting from our target capture approach for various within- and between-species comparisons are apparently the first such data presented for a range of related species of lichen fungi. The data revealed mean identities for within-species comparisons of > 99.5%, whereas between-species identities were consistently below 98.5%. This appears to support the commonly applied approach of fixed similarity thresholds, such as 98.5% for the fungal ITS barcoding marker in the curated UNITE ITS database (Kõljalg *et al.*, 2019). However, the markers analysed through the target capture approach are not comparable to ITS, and between individual markers there were differences for each pairing. Nevertheless, statistical comparison of genetic similarities from a target capture approach appears to be a promising tool to assess the taxonomy of species complexes with discrete phenotype variation, although we expect that RADseq will provide a higher resolution in such cases (Grewe *et al.*, 2018; Widhelm *et al.*, 2021).

ACKNOWLEDGEMENTS

FUNDING

DATA AVAILABILITY

The data underlying this article are available as supplementary information; sequence data have been deposited in GenBank [https://www.ncbi.nlm.nih.gov/genbank] and the Sequence Read Archive [https://www.ncbi.nlm.nih.gov/sra], as outlined in Tables 1, 2.

CONFLICT OF INTEREST

The authors declare no conflict of interest.

REFERENCES

Armaleo D, Clerc P. 1991. Lichen chimeras: DNA analysis suggests that one fungus forms two morphotypes. *Experimental Mycology* **15:** 1–10.

Articus K, **Mattsson JE**, **Tibell L**, **Grube M**, **Wedin M. 2002.** Ribosomal DNA and β-tubulin data do not support the separation of the lichens *Usnea florida* and *U. subfloridana* as distinct species. *Mycological Research* **106:** 412–418.

Baldwin BG, **Kyhos DW**, **Dvorak J**, **Carr GD. 1991.** Chloroplast DNA evidence for a North American origin of the Hawaiian silversword alliance (Asteraceae). *Proceedings of the National Academy of Sciences, USA* **88:** 1840–1843.

Baldwin BG, **Sanderson MJ. 1998.** Age and rate of diversification of the Hawaiian silversword alliance (Compositae). *Proceedings of the National Academy of Sciences, USA* **95:** 9402–9406.

Boluda CG, **Rico VJ**, **Divakar PK**, **Nadyeina O**, **Myllys L**, **McMullin RT**, **Zamora JC**, **Scheidegger C**, **Hawksworth DL. 2019.** Evaluating methodologies for species delimitation: the mismatch between phenotypes and genotypes in lichenized fungi (*Bryoria* sect. *Implexae*, Parmeliaceae). *Persoonia* **42:** 75–100.

Buschbom J, **Mueller GM. 2006.** Testing "species pair" hypotheses: evolutionary processes in the lichen-forming species complex *Porpidia flavocoerulescens* and *Porpidia melinodes*. *Molecular Biology and Evolution* **23:** 574–586.

Carlquist S, Baldwin BG, Carr GD, eds. 2003. *Tarweeds & silverswords: evolution of the Madiinae (Asteraceae)*. St. Louis: Missouri Botanical Garden Press.

Chamala S, **García N**, **Godden GT**, **Krishnakumar V**, **Jordon-Thaden IE**, **De Smet R**, **Barbazuk WB**, **Soltis DE**, **Soltis PS. 2015.** MarkerMiner 1.0: a new application for phylogenetic marker development using angiosperm transcriptomes. *Applications in Plant Sciences* **3:** 1400115.

Chevin LM, **Hoffmann AA. 2017.** Evolution of phenotypic plasticity in extreme environments. *Philosophical Transactions of the Royal Society B: Biological Sciences* **372:** 20160138.

Chevin LM, **Lande R. 2013.** Evolution of discrete phenotypes from continuous norms of reaction. *The American Naturalist* **182:** 13–27.

Clement M, **Snell Q**, **Walker P**, **Posada D**, **Crandall K. 2002.** TCS: estimating gene genealogies. *International Parallel and Distributed Processing Symposium* **2:** 184.

Coissac E, **Hollingsworth PM**, **Lavergne S**, **Taberlet P. 2016.** From barcodes to genomes: extending the concept of DNA barcoding. *Molecular Ecology* **25:** 1423–1428.

Cornejo C, **Scheidegger C. 2015.** Multi-gene phylogeny of the genus *Lobaria*: evidence of species-pair and allopatric cryptic speciation in East Asia. *American Journal of Botany* **102:** 2058–2073.

Crespo A, **Pérez-Ortega S. 2009.** Cryptic species and species pairs in lichens: a discussion on the relationship between molecular phylogenies and morphological characters. *Anales del Jardín Botánico de Madrid* **66:** 71–81.

Crous PW, **Braun U**, **Hunter GC**, **Wingfield MJ**, **Verkley GJ**, **Shin HD**, **Nakashima C**, **Groenewald JZ. 2013.** Phylogenetic lineages in *Pseudocercospora*. *Studies in Mycology* **75:** 37–114.

Devkota S, **Keller C**, **Olley L**, **Werth S**, **Chaudhary RP**, **Scheidegger C. 2017.** Distribution and national conservation status of the lichen family Lobariaceae (Peltigerales): from subtropical luxuriant forests to the alpine scrub of Nepal Himalaya. *Mycosphere* **8:** 630–648.

Doré CJ, **Cole MS**, **Hawksworth DL. 2006.** Preliminary statistical studies of the infraspecific variation in the ascospores of *Nesolechia oxyspora* growing on different genera of parmelioid lichens. *The Lichenologist* **38:** 425–434.

Eberhardt U. 2010. A constructive step towards selecting a DNA barcode for fungi. *The New Phytologist* **187:** 265–268.

AQ34

Ekman S, **Tønsberg T**, **Jørgensen PM. 2019.** The *Sticta fuliginosa* group in Norway and Sweden. *Graphis Scripta* **31:** 23–33.

Ertz D, **Guzow-Krzemińska B**, **Thor G**, **Łubek A**, **Kukwa M. 2018.** Photobiont switching causes changes in the reproduction strategy and phenotypic dimorphism in the Arthoniomycetes. *Scientific Reports* **8:** 4952.

Frisvad JC. 1992. Chemometrics and chemotaxonomy: a comparison of multivariate statistical methods for the evaluation of binary fungal secondary metabolite data. *Chemometrics and Intelligent Laboratory Systems* **14:** 253–269.

Fryday AM, **Schmit I**, **Pérez-Ortega S. 2017.** The genus *Endocena* (Icmadophilaceae): DNA evidence suggests the same fungus forms different morphologies. *The Lichenologist* **49:** 347–363.

Futuyma DJ. 2015. Can modern evolutionary theory explain macroevolution? In: Serrelli E, Gontier N, eds. *Macroevolution*. Cham: Springer, 29–85.

Galloway DJ. 1985. *Flora of New Zealand lichens*. Wellington: Hasselberg Government Printer.

Galloway DJ. 1997. Studies on the lichen genus *Sticta* (Schreber) Ach. IV. New Zealand species. *The Lichenologist* **29:** 105–168.

Galloway DJ. 2007. *Flora of New Zealand lichens. Vol. 1. Revised 2nd ed.* Lincoln: Manaaki Whenua Press.

Galloway DJ, **Stenroos S**, **Ferraro LI. 1995.** *Flora criptogámica de Tierra del Fuego. Lichenes, Peltigerales: Lobariaceae y Stictaceae. Vol. 6, Fasc. 6.* Buenos Aires: Consejo Nacional de Investigaciones Cientificas y Técnicas de la República Argentina.

Garnier S. 2016. *Viridis: default color maps from "matplotlib". R Package, version* 0.3.4. Available at: https://rdrr.io/cran/viridis/

Glenn TC, **Nilsen RA**, **Kieran TJ**, **Sanders JG**, **Bayona-Vásquez NJ**, **Finger JW**, **Pierson TW**, **Bentley KE**, **Hoffberg SL**, **Louha S**, **Garcia-De Leon FJ**, **Del Rio Portilla MA**, **Reed KD**, **Anderson JL**, **Meece JK**, **Aggrey SE**, **Rekaya R**, **Alabady M**, **Belanger M**, **Winker K**, **Faircloth BC. 2019.** Adapterama I: universal stubs and primers for 384 unique dual-indexed or 147,456 combinatorially-indexed Illumina libraries (iTru & iNext). *PeerJ* **7:** e7755.

Goward T. 2009. VII. Species. *Evansia* **26:** 153–162.

Grabherr MG, **Haas BJ**, **Yassour M**, **Levin JZ**, **Thompson DA**, **Amit I**, **Adiconis X**, **Fan L**, **Raychowdhury R**, **Zeng Q**, **Chen Z**, **Mauceli E**, **Hacohen N**, **Gnirke A**, **Rhind N**, **di Palma F**, **Birren BW**, **Nusbaum C**, **Lindblad-Toh K**, **Friedman N**, **Regev A. 2011.** Full-length transcriptome assembly from RNA-Seq data without a reference genome. *Nature Biotechnology* **29:** 644–652.

Greshake B, **Zehr S**, **Dal Grande F**, **Meiser A**, **Schmitt I**, **Ebersberger I. 2016.** Potential and pitfalls of eukaryotic metagenome skimming: a test case for lichens. *Molecular Ecology Resources* **16:** 511–523.

Grewe F, **Lagostina E**, **Wu H**, **Printzen C**, **Lumbsch HT. 2018.** Population genomic analyses of RAD sequences resolves the phylogenetic relationship of the lichen-forming fungal species *Usnea antarctica* and *Usnea aurantiacoatra*. *MycoKeys* **43:** 91–113.

Heiðmarsson S, **Mattsson JE**, **Moberg R**, **Nordin A**, **Santesson R**, **Tibell L. 1997.** Classification of lichen photomorphs. *Taxon* **46:** 519–520.

Högnabba F, **Stenroos S**, **Thell A. 2009.** Phylogenetic relationship and evolution of photobiont associations in the Lobariaceae (Peltigerales, Lecanoromycetes, Ascomycota). *Bibliotheca Lichenologica* **100:** 157–187.

James TY, **Moncalvo JM**, **Li S**, **Vilgalys R. 2001.** Polymorphism at the ribosomal DNA spacers and its relation to breeding structure of the widespread mushroom *Schizophyllum commune*. *Genetics* **157:** 149–161.

Johnson MG, **Gardner EM**, **Liu Y**, **Medina R**, **Goffinet B**, **Shaw AJ**, **Zerega NJ**, **Wickett NJ. 2016.** HybPiper: extracting coding sequence and introns for phylogenetics from high-throughput sequencing reads using target enrichment. *Applications in Plant Sciences* **4:** 1600016.

Jørgensen PM. 1998. What shall we do with the blue-green counterparts? *The Lichenologist* **30:** 351–356.

Katoh K, **Standley DM. 2013.** MAFFT multiple sequence alignment software version 7: improvements in performance and usability. *Molecular Biology and Evolution* **30:** 772–780.

Kearse M, **Moir R**, **Wilson A**, **Stones-Havas S**, **Cheung M**, **Sturrock S**, **Buxton S**, **Cooper A**, **Markowitz S**, **Duran C**, **Thierer T**, **Ashton B**, **Meintjes P**, **Drummond A. 2012.** Geneious Basic: an integrated and extendable desktop software platform for the organization and analysis of sequence data. *Bioinformatics* **28:** 1647–1649.

Kõljalg U, **Abarenkov K**, **Nilsson RH**, **Larsson KH**, **Taylor AF. 2019.** The UNITE database for molecular identification and for communicating fungal species. *Biodiversity Information Science and Standards* **3:** e374.

Kraichak E, **Huang JP**, **Nelsen MP**, **Leavitt SD**, **Lumbsch HT. 2018.** A revised classification of orders and families in the two major subclasses of Lecanoromycetes (Ascomycota) based on a temporal approach. *Botanical Journal of the Linnean Society* **188:** 233–249.

Lagostina E, **Dal Grande F**, **Andreev M**, **Printzen C. 2018.** The use of microsatellite markers for species delimitation in Antarctic *Usnea* subgenus *Neuropogon*. *Mycologia* **110:** 1047–1057.

de Lange PJ. 2014. A revision of the New Zealand *Kunzea ericoides* (Myrtaceae) complex. *PhytoKeys* **40:** 1–185.

de Lange PJ, **Blanchon DJ**, **Knight A**, **Elix JA**, **Lücking R**, **Frogley K**, **Harris A**, **Cooper J**, **Rolfe J. 2018.** *Conservation status of New Zealand indigenous lichens and lichenicolous fungi, 2018. New Zealand Threat Classification Series 27.* Wellington: Department of Conservation.

de Lange PJ, **Galloway DJ. 2015.** Lichen notes from the Kermadec Islands. I. Lobariaceae. *Auckland Museum Bulletin* **20:** 115–137.

Laundon JR. 1995. On the classification of lichen photomorphs. *Taxon* **44:** 387–389.

Leavitt SD, **Divakar PK**, **Crespo A**, **Lumbsch HT. 2016.** A matter of time – understanding the limits of the power of molecular data for delimiting species boundaries. *Herzogia* **29:** 479–492.

Leavitt SD, **Johnson LA**, **Goward T**, **Clair LLS. 2011.** Species delimitation in taxonomically difficult lichen-forming fungi: an example from morphologically and chemically diverse *Xanthoparmelia* (Parmeliaceae) in North America. *Molecular Phylogenetics and Evolution* **60:** 317–332.

Leavitt SD, **Lumbsch HT**, **Stenroos S**, **St Clair LL. 2013.** Pleistocene speciation in North American lichenized fungi and the impact of alternative species circumscriptions and rates of molecular evolution on divergence estimates. *PLoS One* **8:** e85240.

Leigh JW, **Bryant D. 2015.** Popart: full-feature software for haplotype network construction. *Methods in Ecology and Evolution* **6:** 1110–1116.

Li H, **Handsaker B**, **Wysoker A**, **Fennell T**, **Ruan J**, **Homer N**, **Marth G**, **Abecasis G**, **Durbin R**, **1000 Genome Project Data Processing Subgroup**. **2009.** The Sequence Alignment/Map format and SAMtools. *Bioinformatics* **25:** 2078–2079.

Lindgren H, **Moncada B**, **Lücking R**, **Magain N**, **Simon A**, **Goffinet B**, **Sérusiaux E**, **Nelsen MP**, **Mercado-Díaz JA**, **Widhelm TJ**, **Lumbsch HT. 2020.** Cophylogenetic patterns in algal symbionts correlate with repeated symbiont switches during diversification and geographic expansion of lichen-forming fungi in the genus *Sticta* (Ascomycota, Peltigeraceae). *Molecular Phylogenetics and Evolution* **150:** 106860.

Lively CM. 1986. Canalization versus developmental conversion in a spatially variable environment. *The American Naturalist* **128:** 561–572.

Llop E, **Gómez-Bolea A. 1999.** *Bacidia parathalassica* (Bacidiaceae, Lecanorales), a new Mediterranean corticolous lichen. *Mycotaxon* **72:** 79–90.

Lohtander K, **Myllys L**, **Sundin R**, **Källersjö M**, **Tehler A. 1998.** The species pair concept in the lichen *Dendrographa leucophaea* (Arthoniales): analyses based on ITS sequences. *The Bryologist* **101:** 404–411.

Lorimer NG. 2007. *Phylogenetic reconstruction and gene tree incongruence in New Zealand* Epilobium *L. (Onagraceae).* Masters Thesis: University of Auckland.

Lücking R. 2019. Stop the abuse of time! A critical review of temporal banding for rank-based classifications in Fungi (including lichens) and other organisms. *Critical Review in Plant Sciences* **38:** 199–253.

Lücking R, **Hodkinson BP**, **Leavitt SD. 2017b.** The 2016 classification of lichenized fungi in the Ascomycota and Basidiomycota – approaching one thousand genera. *The Bryologist* **119:** 361–416.

Lücking R, **Moncada B**, **McCune B**, **Farkas E**, **Goffinet B**, **Parker D**, **Chaves JL**, **Lőkös L**, **Nelson PR**, **Spribille T**, **Stenroos S**, **Wheeler T**, **Yanez-Ayabaca A**, **Dillman K**, **Gockman OT**, **Goward T**, **Hollinger J**, **Tripp EA**, **Villella J**, **Álvaro-Alba WR**, **Julio Arango C**, **Cáceres MES**, **Fernando Coca L**, **Printzen C**, **Rodríguez C**, **Scharnagl K**, **Rozzi R**, **Soto-Medina E**, **Yakovchenko LS. 2017a.** *Pseudocyphellaria crocata* (Ascomycota: Lobariaceae) in the Americas is revealed to be thirteen species, and none of them is *P. crocata*. *The Bryologist* **120:** 441–500.

Lücking R, **Moncada B**, **Smith CW. 2017c.** The genus *Lobariella* (Ascomycota: Lobariaceae) in Hawaii: late colonization, high inferred endemism and three new species resulting from "micro-radiation". *The Lichenologist* **49:** 673–691.

Ludwig LR. 2011. Marginal soralia and conidiomata in *Icmadophila splachnirima* (Icmadophilaceae) from southern New Zealand. *Australasian Lichenology* **68:** 4–11.

Lumbsch HT, **Leavitt SD. 2011.** Goodbye morphology? A paradigm shift in the delimitation of species in lichenized fungi. *Fungal Diversity* **50:** 59–72.

Lumbsch TH, **Leavitt SD. 2019.** Introduction of subfamily names for four clades in Cladoniaceae and Peltigeraceae (Lecanoromycetes). *Mycotaxon* **134:** 271–273.

Lutzoni FM. 1994. *Ionaspis alba* (Ascomycotina, Hymeneliaceae), a new lichen species from eastern North America. *The Bryologist* **97:** 393–395.

Magain N, **Goffinet B**, **Sérusiaux E. 2012.** Further photomorphs in the lichen family Lobariaceae from Reunion (Mascarene archipelago) with notes on the phylogeny of *Dendriscocaulon* cyanomorphs. *The Bryologist* **115:** 243–254.

Magain N, **Miadlikowska J**, **Mueller O**, **Gajdeczka M**, **Truong C**, **Salamov AA**, **Dubchak I**, **Grigoriev IV**, **Goffinet B**, **Sérusiaux E**, **Lutzoni F. 2017.** Conserved genomic collinearity as a source of broadly applicable, fast evolving, markers to resolve species complexes: a case study using the lichen-forming genus *Peltigera* section *Polydactylon*. *Molecular Phylogenetics and Evolution* **117:** 10–29.

Magain N, **Sérusiaux E. 2015.** Dismantling the treasured flagship lichen *Sticta fuliginosa* (Peltigerales) into four species in western Europe. *Mycological Progress* **14:** 97.

Magain N, **Tniong C**, **Goward T**, **Niu D**, **Goffinet B**, **Sérusiaux E**, **Vitikainen O**, **Lutzoni F**, **Miadlikowska J. 2018.** Species delimitation at a global scale reveals high species richness with complex biogeography and patterns of symbiont association in *Peltigera* section *Peltigera* (lichenized Ascomycota: Lecanoromycetes). *Taxon* **67:** 836–870.

Makryi TV. 2008. Lichens of the genus *Sticta* (Lobariaceae) in Russia. *Botanicheskii Zhurnal* **93:** 304–316.

Mattsson JE, **Lumbsch HT. 1989.** The use of the species pair concept in lichen taxonomy. *Taxon* **38:** 238–241.

McCune B, **Mefford MJ. 2006.** *PC-ORD v5. Multivariate analysis of ecological data*. Gleneden Beach: MjM Software.

Messuti MI, **Passo A**, **Scervino JM**, **Vidal-Russell R. 2016.** The species pair *Pseudocyphellaria pilosella-piloselloides* (lichenized Ascomycota: Lobariaceae) is a single species. *The Lichenologist* **48:** 141–146.

Meudt H, **Prebble J**, **Lehnebach C. 2014.** Native New Zealand forget-me-nots (*Myosotis*, Boraginaceae) comprise a Pleistocene species radiation with very low genetic divergence. *Plant Systematics and Evolution* **301:** 1455–1471

Moncada B, **Lücking R**, **Betancourt-Macuase L. 2013.** Phylogeny of the Lobariaceae (lichenized Ascomycota: Peltigerales), with a reappraisal of the genus *Lobariella*. *The Lichenologist* **45:** 203–263.

Moncada B, **Lücking R**, **Suárez A. 2014a.** Molecular phylogeny of the genus *Sticta* (lichenized Ascomycota: Lobariaceae) in Colombia. *Fungal Diversity* **64:** 205–231.

Moncada B, **Reidy B**, **Lücking R. 2014b.** A phylogenetic revision of Hawaiian *Pseudocyphellaria sensu lato* (lichenized Ascomycota: Lobariaceae) reveals eight new species and a high degree of inferred endemism. *The Bryologist* **117:** 119–160.

Moran NA. 1992. The evolutionary maintenance of alternative phenotypes. *The American Naturalist* **139:** 971–989.

Mugford J, **Moltchanova E**, **Plank M**, **Sullivan J**, **Byrom A**, **James A. 2021.** Citizen science decisions: a Bayesian approach optimises effort. *Ecological Informatics* **63:** 101313.

Muggia L, **Grube M**, **Tretiach M. 2008.** Genetic diversity and photobiont associations in selected taxa of the *Tephromela atra* group (Lecanorales, lichenised Ascomycota). *Mycological Progress* **7:** 147–160.

Muggia L, **Pérez-Ortega S**, **Fryday A**, **Spribille T**, **Grube M. 2014.** Global assessment of genetic variation and phenotypic plasticity in the lichen-forming species *Tephromela atra*. *Fungal Diversity* **64:** 233–251.

Myllys L, **Lohtander K**, **Tehler A. 2001.** β-tubulin, ITS and group I intron sequences challenge the species pair concept in *Physcia aipolia* and *P. caesia*. *Mycologia* **93:** 335–343.

O'Donnell K, **Ward TJ**, **Robert VARG**, **Crous PW**, **Geiser DM**, **Kang S. 2015.** DNA sequence-based identification of *Fusarium*: current status and future directions. *Phytoparasitica* **43:** 583–595.

Oettler J, **Platschek T**, **Schmidt C**, **Rajakumar R**, **Favé MJ**, **Khila A**, **Heinze J**, **Abouheif E. 2019.** Interruption points in the wing gene regulatory network underlying wing polyphenism evolved independently in male and female morphs in *Cardiocondyla* ants. *Journal of Experimental Zoology. Part B, Molecular and Developmental Evolution* **332:** 7–16.

Pizarro D, **Divakar PK**, **Grewe F**, **Leavitt SD**, **Huang JP**, **Dal Grande F**, **Schmitt I**, **Wedin M**, **Crespo A**, **Lumbsch HT. 2018.** Phylogenomic analysis of 2556 single-copy protein-coding genes resolves most evolutionary relationships for the major clades in the most diverse group of lichen-forming fungi. *Fungal Diversity* **92:** 31–41.

Purvis W. 2000. *Lichens.* London: Natural History Museum; Washington: Smithsonian Institution.

Ranft H, **Moncada B**, **de Lange PJ**, **Lumbsch HT**, **Lücking R. 2018.** The *Sticta filix* morphodeme (Ascomycota: Lobariaceae) in New Zealand with the newly recognized species *S. dendroides* and *S. menziesii*: indicators of forest health in a threatened island biota? *The Lichenologist* **50:** 185–210.

Samson RA, **Visagie CM**, **Houbraken J**, **Hong SB**, **Hubka V**, **Klaassen CH**, **Perrone G**, **Seifert KA**, **Susca A**, **Tanney JB**, **Varga J**, **Kocsubé S**, **Szigeti G**, **Yaguchi T**, **Frisvad JC. 2014.** Phylogeny, identification and nomenclature of the genus *Aspergillus*. *Studies in Mycology* **78:** 141–173.

Sanders WB. 2001. Composite lichen thalli of *Sticta* sp. from Brazil, with morphologically similar lobes containing either a chlorobiont or a cyanobiont layer. *Symbiosis* **31:** 47–55.

Shepherd LD, **de Lange PJ**, **Townsend A**, **Perrie LR. 2019.** A biological and ecological review of the endemic New Zealand genus *Alseuosmia* (toropapa; Alseuosmiaceae). *New Zealand Journal of Botany* **58:** 2–18.

Sieber TN, **Petrini O**, **Greenacre MJ. 1998.** Correspondence analysis as a tool in fungal taxonomy. *Systematic and Applied Microbiology* **21:** 433–441.

Sieriebriennikov B, **Prabh N**, **Dardiry M**, **Witte H**, **Röseler W**, **Kieninger MR**, **Rödelsperger C**, **Sommer RJ. 2018.** A developmental switch generating phenotypic plasticity is part of a conserved multi-gene locus. *Cell Reports* **23:** 2835–2843.

Simon A, **Goffinet B**, **Magain N**, **Sérusiaux E. 2018a.** High diversity, high insular endemism and recent origin in the lichen genus *Sticta* (lichenized Ascomycota, Peltigerales) in Madagascar and the Mascarenes. *Molecular Phylogenetics and Evolution* **122:** 15–28.

Simon A, **Goward T**, **Di Meglio J**, **Dillman K**, **Spribille T**, **Goffinet B. 2018b.** *Sticta torii* sp. nov., a remarkable lichen of high conservation priority from northwestern North America. *Graphis Scripta* **30:** 105–114.

Simon A, **Lücking R**, **Moncada B**, **Mercado-Díaz JA**, **Bungartz F**, **Cáceres MES**, **Gumboski EL**, **Martins SMA**, **Spielmann AA**, **Parker D**, **Goffinet B. 2020.** *Emmanuelia*, a new genus of lobarioid lichen-forming fungi (Ascomycota: Peltigerales): phylogeny and synopsis of accepted species. *Plant and Fungal Systematics* **65:** 76–94.

Sneath PH, **Sokal RR. 1973.** *Numerical taxonomy. The principles and practice of numerical classification.* San Francisco: Freeman & Co.

Stamatakis A. 2015. Using RAxML to infer phylogenies. Unit 6.14. *Current Protocols in Bioinformatics* **51:** 1–6.

Stenroos S, **Stocker-Wörgötter E**, **Yoshimura I**, **Myllys L**, **Thell A**, **Hyvönen J. 2003.** Culture experiments and DNA sequence data confirm the identity of *Lobaria* photomorphs. *Canadian Journal of Botany* **81:** 232–247.

Takahashi K, **Wang LS**, **Tsubota H**, **Deguchi H. 2006.** Photosymbiodemes *Sticta wrightii* and *Dendriscocaulon* sp. (lichenized Ascomycota) from Yunnan, China. *Journal of the Hattori Botanical Laboratory* **100:** 783–796.

Tehler A. 1982. The species pair concept in lichenology. *Taxon* **31:** 708–714.

Thomas MA, **Ryan DJ**, **Farnden KJF**, **Galloway DJ. 2002.** Observations on phylogenetic relationships within Lobariaceae Chevall. (Lecanorales, Ascomycota) in New Zealand, based on ITS-5.8S molecular sequence data. *Bibliotheca Lichenologica* **82:** 123–138.

Tønsberg T, **Goward T. 2001.** *Sticta oroborealis* sp. nov. and other Pacific North American lichens forming dendriscocauloid cyanotypes. *The Bryologist* **104:** 12–23.

Tønsberg T, **Holtan-Hartwig J. 1983.** Phycotype pairs in *Nephroma*, *Peltigera* and *Lobaria* in Norway. *Nordic Journal of Botany* **3:** 681–688.

Tønsberg T, **Blom HH**, **Goffinet B**, **Holtan-Hartwig J**, **Lindblom L. 2016.** The cyanomorph of *Ricasolia virens*

comb. nov. (Lobariaceae, lichenized Ascomycetes). *Opuscula Philolichenum* **15:** 12–21.

Tretiach M, **Hafellner J. 1998.** A new species of *Catillaria* from coastal Mediterranean regions. *The Lichenologist* **30:** 221–229.

Weigel D, **Nilsson O. 1995.** A developmental switch sufficient for flower initiation in diverse plants. *Nature* **377:** 495–500.

West-Eberhard MJ. 2003. *Developmental plasticity and evolution*. New York: Oxford University Press.

Wickham H. 2016. *ggplot2: elegant graphics for data analysis.* New York: Springer.

Wickham H, **Francois R**, **Henry L**, **Müller K. 2015.** *dplyr: a grammar of data manipulation. R Package, version 0.4 3.* Available at: https://dplyr.tidyverse.org

Widhelm TJ, **Bertoletti FR**, **Asztalos MJ**, **Mercado-Díaz JA**, **Huang JP**, **Moncada B**, **Lücking R**, **Magain N**, **Sérusiaux E**, **Goffinet B**, **Crouch N**, **Mason-Gamer R**, **Lumbsch HT. 2018.** Oligocene origin and drivers of diversification in the genus *Sticta* (Lobariaceae, Ascomycota). *Molecular Phylogenetics and Evolution* **126:** 58–73.

Widhelm TJ, **Grewe F**, **Huang JP**, **Mercado-Díaz JA**, **Goffinet B**, **Lücking R**, **Moncada B**, **Mason-Gamer R**, **Lumbsch HT. 2019.** Multiple historical processes obscure phylogenetic relationships in a taxonomically difficult group (Lobariaceae, Ascomycota). *Scientific Reports* **9:** 8968.

Widhelm TJ, **Grewe F**, **Huang JP**, **Ramanauskas K**, **Mason-Gamer R**, **Lumbsch HT. 2021.** Using RADseq to understand the circum-Antarctic distribution of a lichenized fungus, *Pseudocyphellaria glabra*. *Journal of Biogeography* **48:** 78–90.

Wilke CO. 2017. *Ggridges: Ridgeline plots in ggplot2. R Package, version 0.4 1.* Available at: https://cran.r-project.org/web/packages/ggridges/vignettes/introduction.html

SUPPORTING INFORMATION

Additional Supporting Information may be found in the online version of this article at the publisher's web-site:

Table S1. Morphometrical assessment of specimens of *S. filix* and *S. lacera*. In *S. lacera*, the column 'Stem length [mm]' refers to the lateral stems emerging from the proliferating basal stem and so correspond to the side branches in *S. filix*.

Table S2. Assessment of ecological data (substrate) of samples of *S. filix* and *S. lacera* based on field images posted on iNaturalist NZ (accessed 17 May 2021). The corresponding species-level links bundling the individual postings are https://inaturalist.nz/observations?taxon_id=197044 (*S. filix*) and https://inaturalist.nz/observations?taxon_id=408333 (*S. lacera*). Of the 92 postings originally identified as *S. filix*, 27 did not represent that species, leaving 65 verified records; of the 22 postings originally identified as *S. lacera*, nine did not represent that species, leaving 13 verified records.

File S3. Individual alignments (in FASTA format) of the 205 markers used from the target capture approach.